Geoderma 436 (2023) 116549

Contents lists available at ScienceDirect

Geoderma

journal homepage: www.elsevier.com/locate/geoderma

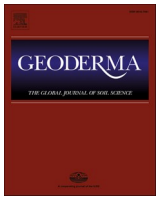

Potential of soil minerals to sequester soil organic carbon

Heidy Soledad Rodríguez-Albarracín [a], José A.M. Demattê [a,*], Nícolas Augusto Rosin [a], Aquiles Enrique Darghan Contreras [b], Nélida E.Q. Silvero [a], Carlos Eduardo Pellegrino Cerri [a], Wanderson de Sousa Mendes [c], Mahboobeh Tayebi [d]

[a] Departament of Soil Science, Luiz de Queiroz College of Agriculture (ESALQ), University of São Paulo (USP), Piracicaba, São Paulo, Zip Code: 13418-900, Brazil
[b] Faculty of Agriculture Sciences, Department of Agronomy, Universidad Nacional de Colombia, Carrera 30 núm. 45-03, Building 500, Bogotá DC, Colombia
[c] Leibniz Centre for Agricultural Landscape Research (ZALF), "Landscape Pedology" Working Group, Reasearch Area 1 "Landscape Functioning", 15374 Müncheberg, Germany
[d] Soil and Water Sciences Department, University of Florida, McCarty Hall, Gainesville, FL 32611, USA

ARTICLE INFO

Handling Editor: Jingyi Huang

Keywords:
Spatial regression
Digital soil mapping
Sustainability
Soil security
Soil spectroscopy
Saturation deficit

ABSTRACT

The capacity of soil to sequester carbon (C) is a key process that promotes the reduction of CO_2 in the atmosphere. Soils can absorb as much as 20% of anthropogenic carbon emissions, which can contribute to mitigate climate change. This capacity relies on the organo-mineral association, which includes different minerals, Fe and Al oxides, which have a critical soil organic carbon (SOC) sorption surface. Based on an equation of the potential C saturation deficit of fine soil particles (<20 μm/silt and clay fractions) for tropical regions, this study investigated the SOC sequestration potential of the clay fraction for soils in Piracicaba region, São Paulo State, Brazil as influenced by the clay minerals. This potential was fitted to a spatial regression model for soil depths 0–20 cm and 80 to 100 cm. In the surface layer, the sequestration potential was mostly explained by the relative abundance of soil minerals (Kaolinite, Hematite, Goethite and Gibbsite) determined using vis-NIR-SWIR spectroscopy. A direct relationship was observed with Goethite and Gibbsite, indicating that low concentrations would reduce the sequestration potential. At 80 to 100 cm depth, Kaolinite and Hematite explained most variation in SOC sequestration potential. Additionally, the C associated with the mineral fraction and the C saturation potential as a function of minerals were modeled and a strong importance of hematite in the C sequestration and stabilization cycle was identified at both depths. The individual mineral contribution to SOC sequestration potential was also mapped, which identified high contributions of goethite and gibbsite for deep soil layers. The influence of land use on the carbon sequestration potential of minerals was observed, with the greatest potential being found in areas with pasture and cropping mosaics and grassland and forest mosaics, with a high presence of kaolinite and hematite. These minerals have a greater potential for carbon sequestration at greater depths and, therefore, could be critical in climate change mitigation strategies.

1. Introduction

The ability of soil to sequester carbon is considered a cost-effective and plausible method to reduce the concentration of CO_2 in the atmosphere (Houghton, 2003, Kimble et al., 2003). This is because global soils have the potential to absorb about 20% of anthropogenic carbon emissions (Yang et al., 2021). Therefore, carbon sequestration is a phenomenon that can help to partially mitigate climate change (Padarian et al., 2022), as for greenhouse gas emissions (Minasny et al., 2017).

Hassink (1997) and Loveland and Webb (2003) proposed that soils have a limited capacity to retain carbon, which is based on the reactive capacity of mineral surfaces (Churchman et al., 2020; Prout et al., 2021). Therefore, it is understood that the clay fraction has a finite carbon storage capacity (Diekow et al., 2005), and the search for this storage limit justifies the determination of carbon sequestration potential (Six et al., 2002; Stewart et al., 2008; Chung et al., 2008), which also depends on the limited potential of the soil to stabilize soil organic carbon (SOC)

* Corresponding author.
E-mail addresses: hsrodrigueza@usp.br (H.S. Rodríguez-Albarracín), jamdemat@usp.br (J.A.M. Demattê), narosin@usp.br (N.A. Rosin), aqedarghanco@unal.edu.co (A.E.D. Contreras), neli.silvero@usp.br (N.E.Q. Silvero), cepcerri@usp.br (C.E.P. Cerri), wanderson.mendes@zalf.de (W.S. Mendes), mtayebi@ufl.edu (M. Tayebi).

https://doi.org/10.1016/j.geoderma.2023.116549
Received 22 November 2022; Received in revised form 25 May 2023; Accepted 26 May 2023
Available online 2 June 2023

against microbial mineralization.

The SOC stabilization is based on selective preservation associated with recalcitrance or chemical resistance (Singh et al., 2018). It is also related to the spatial inaccessibility of SOM by occlusion in soil aggregates, especially in microaggregates (Hoffland et al., 2020). Furthermore, the interaction with mineral surfaces favors the formation of organic-mineral complexes (Sollins et al., 1996, Von Lützow et al., 2006), especially with clay minerals and metal ions (Oades, 1988, Arrouays et al., 2006, Singh et al., 2018).

Hassink (1997) indicated that the potential carbon saturation is associated with silt and clay particles. Angers et al. (2011) also pointed out that fine-textured soils have a higher retention capacity than sandy soils, due to a larger specific surface area available for organo-mineral interactions present in the silt and clay fractions (Stewart et al., 2008). Similarly, Zeraatpishe and Khormali (2012) observed that the SOC can be adsorbed by coarse aggregates, fine aggregates, and particles smaller than 0.053 mm. Brodowski et al. (2006) found that particles such as clay and silt alone cannot retain much SOC, and more than 90% is stored in the aggregates, which protects SOC from microbial decomposition (Hoffland et al., 2020, Baldock and Skjemstad, 2000, Lützow et al., 2006).

The SOC dynamics is closely related to the soil development process and, therefore, to its formation factors (Hobley et al., 2015). There are active factors, such as climate and organisms, and passive factors, such as parent materials, relief, and time. To make predictions of the terrestrial carbon cycle, it is necessary to understand the complete processes related to the sequestration and release of carbon (Marschner et al., 2008).

Ingram and Fernandes (2001) and Weil and Brady (2016) indicated the importance of mineralogy on the potential for SOC storage, especially soils in the deeper layers (Gray et al., 2015, Wiesmeier et al., 2011). In contrast, land use presents a more significant influence in the superficial layers (Adhikari et al., 2014, Hobley et al., 2015). For Ashton et al. (2016), clay content alone is not related to the increase or decrease of carbon content. The concentration is influenced by soil mineralogy and the geochemistry of the soil, thus depending on the presence of clay minerals and iron oxides of high specific surface area and pH. The clay fraction is key to carbon sequestration because it involves different minerals and varying amounts of pedogenic Fe and Al oxides (Yang et al., 2021; Kirsten et al., 2021; Prout et al., 2021). Minerals such as iron and aluminum oxides, specifically goethite and gibbsite are recognized as critical carbon sorption surfaces (Kaiser and Zech, 2000; Dos Reis et al., 2014).

Feng et al. (2005) highlighted the adsorption of anionic cations by soil organic matter through ionic linkages related to hydrogen, cation and anion exchange, ligand exchange and cation bridges, likewise electrostatic attractions or van der Waals linkages alone can occur. Soil oxides, oxyhydroxides and hydroxides present electrostatic attractions and ionic linkages between the hydroxyl groups of the oxides and the carboxyl or hydroxyl groups of the SOM, with additional strong relationships between iron manganese and humic substances (De Mastro et al., 2020). This adsorption of SOM by minerals favors SOC stabilization, reducing microbial mineralization (Kalbitz et al., 2005), due to the specific surface area of these minerals and their surface charge that favors these linkages and stabilizes SOM.

Interactions of the reactive phases of poorly crystalline Fe and Al oxides with SOM are an essential mechanism in the long-term stabilization of SOC (Kögel-Knabner et al., 2008, Percival et al., 2000). According to Weber et al. (2006), the biogeochemical cycling of iron is closely related to the dynamics of SOM. Lalonde et al. (2012) noted that about 21.5% of global SOC is associated with reactive forms of Fe. Crystalline Fe and Al oxides present reactive sites on the surface that can adsorb SOC (De Mastro et al., 2020), however Duiker et al. (2003) and De Mastro et al. (2020) observed that Fe oxides of low degree of crystallinity stabilize SOM more effectively than crystalline Fe oxides or oxyhydroxides, because they present higher specific surface area and density of hydroxyl sites compared to crystalline ones, increasing their chelation capacity (Wen et al., 2019). Zeraatpishe and Khormali (2012), to the contrary, reported that amorphous and crystalline iron oxides and hydroxides retain 50–70% of total carbon.

Poorly crystalline Fe minerals have a specific surface area of around 800 $m^2\ g^{-1}$, for example, for ferrihydrite, higher than crystalline forms of Fe found around 200 $m^2\ g^{-1}$, as in the case of goethite (Eusterhues et al., 2005). According to Churchman and Velde (2019), SOC shows a preference for weakly crystalline oxides as well as Fe and Al silicates. Bonds with 2:1 phyllosilicates are going to depend on their relative surface reactivities. Therefore, minerals such as smectite that are more reactive present greater potential to retain carbon (Churchman et al., 2020). However, a more significant effect occurs with poorly crystalline Fe oxyhydroxides (Rasmussen et al., 2007). The combined effect of silicates and oxides is involved in SOC stabilization, for example, ferrihydrite and goethite can favor the sorption capacity of kaolinite (De Mastro et al., 2020).

Kirsten et al. (2021) indicated that clay minerals and oxyhydroxides (pedogenic metal oxides) are the most reactive and control the persistence of SOC. However, most studies did not explicitly evaluate the contribution of clay minerals on SOC. For example, Weismeier et al. (2013) estimated the SOC sequestration potential of silt and clay particles, in soils from Germany, without specifying the clay mineral type. Ashton et al. (2016) analyzed SOC concentrations in different parent materials and clay mineralogies, evaluating total concentrations without determining the specific contribution of each mineral. Yang et al. (2021) evaluated the spatio-temporal dynamics of carbon adsorption and release in aggregates of a transparent smectite clay, also relating enzymatic decomposition, through 4D imaging on a microfluidic chip. It should be noted that this study was not performed on a specific soil. Kirsten et al. (2021) determined the contribution of kaolinite, gibbsite, goethite, and hematite to carbon storage in soils under forests and agricultural lands, evaluating only the variation of carbon and clay mineral concentrations, but keeping the mineral types invariant.

Mapping the carbon sequestration potential that clay minerals composing the clay fraction has is important for the understanding of their dynamics and soil management (Padarian et al., 2022), remembering that SOC contents and their stable forms vary in relation to the amount and type of mineral (Yang et al., 2021; Kirsten et al., 2021; Prout et al., 2021; Dos Reis et al., 2014). However, in general, soil mapping has limitations in terms of spatial delimitation (Teng et al., 2018), and depends on the estimation and description of their properties. These conventional methods require complex laboratory chemical analysis and expertise for their description, incurring more time and costs (Shi et al., 2015), and are generally developed with limited information on quantity, volume and spatial coverage (Soil Survey Staff, 2017).

Information systems and remote sensing techniques have facilitated the acquisition of spatial information, specifically by digital soil mapping (DSM) approaches, which combine point soil data with statistically correlated auxiliary data (covariates) (McBratney et al., 2003), mainly through machine learning techniques (Padarian et al., 2019). Additionally, reflectance spectroscopy is a technology that has improved DSM (Teng et al., 2018), as the evaluation of infrared spectral curves provides useful indicators to map, classify and monitor different soil properties (Di Iorio et al., 2019), as is the case of mineral quantification (Mendes et al., 2021).

This study has the objective of analyzing the individual contribution of each mineral that composes the clay fraction in the sequestration potential of new SOC, through the quantification, modeling and mapping of this potential in different pedogenetic soils of Brazil, using remote sensing products and the equation of Feller and Beare (1997) to obtain the theoretical SOC sequestration potential. Considering the importance of the minerals that compose the clay fraction and that this fraction in tropical soils is dominated by kaolinite, gibbsite, hematite and goethite (Kämpf and Curi, 2003, Schaefer et al., 2008) and the high sorption power of Fe and Al oxides for organic molecules, it is expected

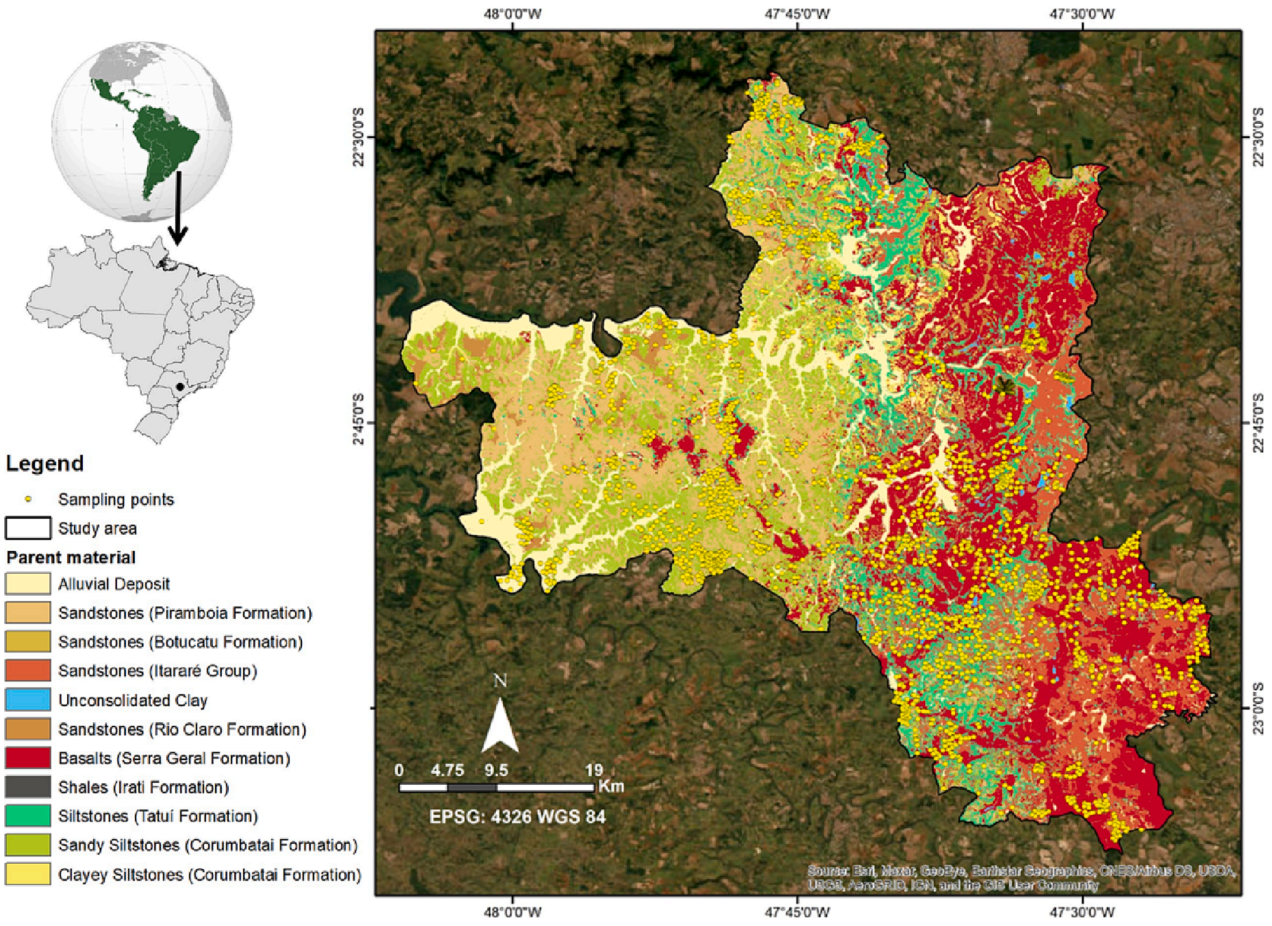

Fig. 1. Location of the study area (Piracicaba region, São Paulo state). The geology map is from Bonfatti et al. (2020).

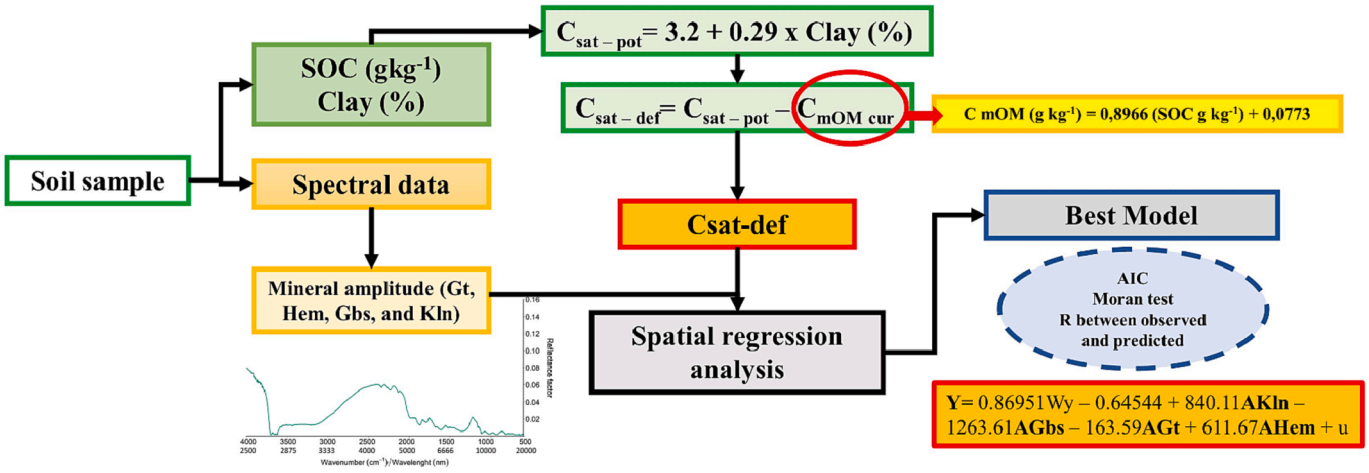

Fig. 2. Methodological scheme of the point modeling of the carbon sequestration potential of minerals that compose the clay fraction. sat-pot: potential C saturation, sat-def: C saturation deficit, CmOM cur: actual concentration of C in mineral-associated organic matter, Gt: goethite, Hem: hematite, Gbs: gibbsite, Kln: kaolinite, A: relative abundance of soil minerals.

that the SOC sequestration potential is directly related to the concentration of these minerals.

2. Methodology

2.1. Study area

The study area is in Piracicaba region, São Paulo State, Brazil, with approximately 2,598 km^2 (Fig. 1). The climate of the region, according to the Köppen system, is classified as subtropical Cwa, with a dry winter and a rainy summer, with an average annual temperature ranging from 20 to 22.5° C and annual rainfall between 1200 and 1400 mm (Alvares et al., 2013). In relation to the topography, undulating highlands and rolling hills with altitudes ranging from 450 to 950 m are characteristic. Agricultural land uses such as sugarcane and pasture are dominant under no-till and conventional tillage management systems. The main

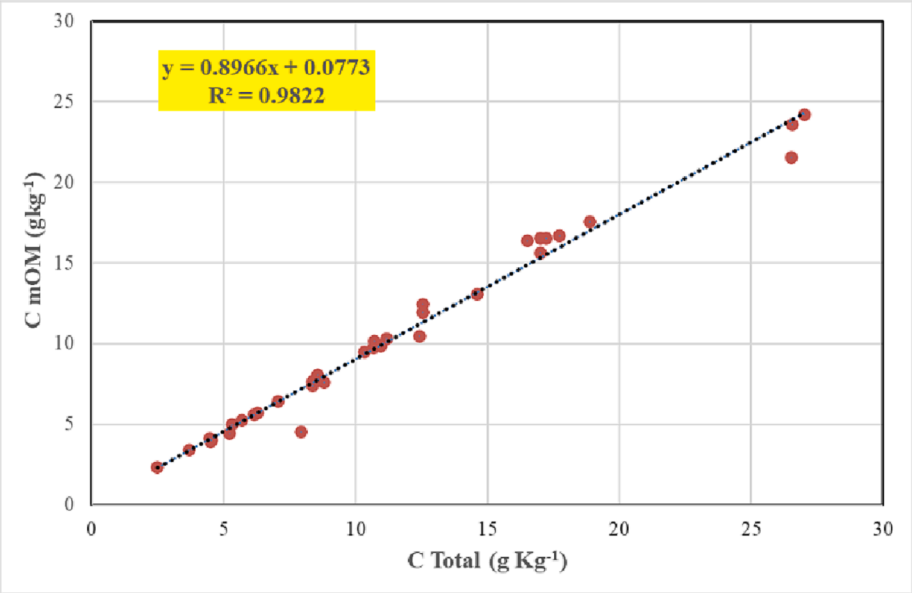

Fig. 3. Simple linear regression between total soil C (x-axes) and C in organic matter associated with the mineral fraction (mOM) (y-axes).

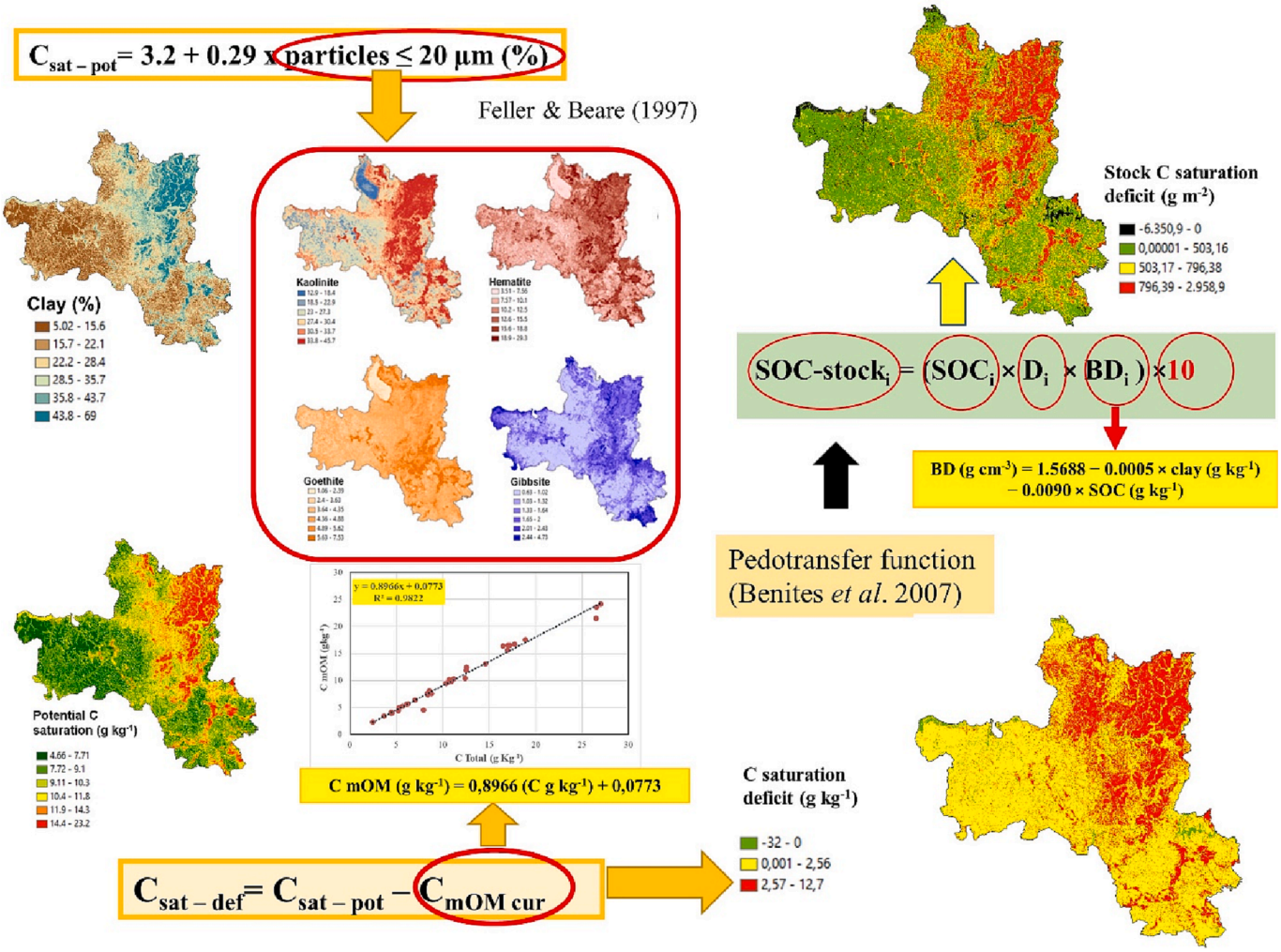

Fig. 4. Methodological scheme for the spatialization of the carbon sequestration potential of the minerals that compose the clay fraction, based on map algebra.

Table 1
Fitted spatial regression models and its related statistics for potential saturation deficit of SOC (Sat-def). λ = autoregressive parameters, ρ = spatial autocorrelation coefficient, r = correlation coefficient, MIT = Moran Index test.

Model	λ	ρ	AIC	r	MIT	Explanatory variables
			0–20 cm			
PAR	0.98 (2.22E^{-16})		6848	0.51	6.41E^{-13}	Sat-def-a
SEM	0.97 (2.22E^{-16})		6708	0.56	2.15E^{-08}	AKln + AGbs + AGt + AHem
SLM		0.95 (2.22E^{-16})	6720	0.55	1.53E^{-10}	AKln + AGbs + AGt + AHem
SLMA		0.97 (2.22E^{-16})	6700	0.56	9.90E^{-06}	AKln + AGbs + AGt + AHem
SARAR	**0.87 (7.53E^{-13})**	**0.66 (7.18E^{-04})**	**6692**	**0.56**	**0.39407**	AKln + AGbs + AGt + AHem
SDEM	0.97 (2.22E^{-16})		6701	0.56	2.98E^{-05}	AKln + AGbs + AGt + AHem
			80–100 cm			
PAR	0.99 (2.22E^{-16})		4520	0.62	2.00E^{-15}	Sat-def-c
SEM	0.98 (2.22E^{-16})		4455	0.65	1.98E^{-10}	AKln + AGbs + AGt + AHem
SLM		0.98 (2.22E^{-16})	4445	0.65	1.65E^{-06}	AKln + AGbs + AHem
SLMA		0.96 (2.22E^{-16})	4443	0.65	3.98E^{-05}	AKln + AGbs + AGt + AHem
SARAR	**0.82 (4.88E-02)**	**0.85 (1.21E^{-02})**	**4429**	**0.66**	**0.37**	AKln + AHem
SDEM	0.98 (2.22E^{-16})		4449	0.65	1.15E^{-07}	AKln + AGbs + AGt + AHem

soil types are Cambisol, Gleysol, Ferralsol, Nitosol, Lixisol, Leptsol, Arenosol and Planosol, according to the World Reference Base (IUSS Working Group WRB, 2015). Geologically, there are diverse parent materials, such as siltstones, tillites, varvites, conglomerates, sandstones, limestones, siltstones, flint, dolomite, siltite, pyrombetuminosite, schists, diabase, and basalt (Bonfatti et al., 2020).

The soil observations used are from the Brazilian Soil Spectral Library (BSSL) (Demattê et al., 2019). A total of 2354 observations from 0 to 20, 40 to 60, and 80 to 100 cm depths were used (Fig. 1). The soil organic carbon (SOC) content and particle size were analyzed by the Walkey-Black method (wet digestion) (Walkey and Black, 1934) and the hydrometer method (Bouyoucus and John, 1962), respectively.

2.2. Point modeling of soil carbon sequestration potential

2.2.1. Carbon saturation potential

Hassink (1997) proposed the following equation to determine the C saturation potential of fine soil particles (<20 μm/silt and clay fractions):

$$C_{sat\text{-}pot} = 4.09 + 0.37 * \text{Particles} \leq 20\ \mu m\ (\%)$$

where $C_{sat\text{-}pot}$ corresponds to the potential carbon saturation (mg g^{-1}), referred to as the theoretical maximum SOC that is stabilized in fine particles and allows estimating the SOC storage potential (Fujisaki et al., 2018). However, considering the study area, the modified

Table 2
Fitted spatial regression models and its related statistics for C in organic matter associated with the mineral fraction (CmOM) and Potential carbon saturation (Sat-pot). λ = autoregressive parameters, ρ = spatial autocorrelation coefficient, r = correlation coefficient, MIT = Moran Index test.

Model	λ	ρ	AIC	r	MIT	Explanatory variables
			C in organic matter associated with the mineral fraction (CmOM)			
			0–20 cm			
PAR	0.98 (2.22E^{-16})		6823.3	0.56	0	CmOM-a
SEM	0.99 (2.22E^{-16})		6700.3	0.59	0	AKln + AGbs + AGt + AHem
SLM		0.98 (2.22E^{-16})	6695.5	0.59	2.87E^{-15}	AKln + AGbs + AGt + AHem
SLMA		0.98 (2.22E^{-16})	6693.1	0.59	2.31E^{-11}	AKln + AGbs + AGt + AHem
SARAR	**0.88 (0.015)**	**0.88 (0.013)**	**6659.1**	**0.60**	**0.1723**	AKln + AGbs + AGt + AHem
			80–100 cm			
PAR	0.99 (2.22E^{-16})		3895.2	0.64	0	CmOM -c
SEM	0.99 (2.22E^{-16})		3783.8	0.68	0	AGbs + AGt + AHem
SLM		0.98 (2.22E^{-16})	3783.7	0.67	0	AGbs + AGt + AHem
SLMA		0.98 (2.22E^{-16})	3778.9	0.68	0	AGbs + AGt + AHem
SARAR	**0.94 (1.59E-06)**	**0.92 (1.60E^{-04})**	**3734.3**	**0.70**	**5.05E^{-02}**	AGbs + AGt + AHem
			Potential carbon saturation (Sat-pot)			
			0–20 cm			
PAR	0.99 (2.22E^{-16})		7053.1	0.65	0	Sat-pot-a
SEM	0.99 (2.22E^{-16})		6620	0.75	0	AKln + AHem
SLM		0.89 (2.22E^{-16})	6623.9	0.74	1.15E^{-14}	AKln + AHem
SLMA		0.98 (2.22E^{-16})	6610.6	0.43	4.68E^{-11}	AKln + AHem
SARAR	**0.89 (2.22E^{-16})**	**0.71 (1.05E^{-07})**	**6586.9**	**0.76**	**0.28**	AKln + AHem
			80–100 cm			
PAR	0.99 (2.22E^{-16})		4711.8	0.75	0	Sat-pot-c
SEM	0.99 (2.22E^{-16})		4517.5	0.79	0	AKln + AGbs + AHem
SLM		0.98 (2.22E^{-16})	4501.1	0.79	1.57E^{-08}	AKln + AGbs + AHem
SLMA		0.99 (2.22E^{-16})	4534.2	0.79	0	AKln + AGbs + AHem
SARAR	**0.86 (8.54E-05)**	**0.86 (9.14E^{-06})**	**4481.5**	**0.66**	**0.37**	AKln + AGbs + AHem

Table 3
Parameters of the SARAR spatial regression model for depths 0 to 20 cm and 8 to 100 cm for potential saturation deficit of SOC (Sat-def).

Coefficients	Estimate	Asymptotic Std. Error	z value	Pr(>|z|)	Impact Direct	Impact p-value
			0–20 cm			
(Intercept)	−0.64	0.89	−0.72	0.47		
AKln	840	142	5.92	**3.26E^{-09}**	**845**	**1.90E^{-09}**
AGbs	−1264	376	−3.35	0.000786	−1272	0.000563
AGt	−164	40	−4.08	4.48E^{-05}	−165	2.94E^{-05}
AHem	612	90	6.80	**1.02E^{-11}**	**616**	**6.10E^{-13}**
			80–100 cm			
(Intercept)	−1.66	1.28	−1.30	0.19		
AKln	600	101	5.94	**2.92E^{-09}**	**611**	**2.72E^{-08}**
AHem	127	66.9	1.90	**0.05**	**130**	**3.35E^{-02}**

Table 4
Parameters of the SARAR spatial regression model for depths 0 to 20 cm and 8 to 100 cm for C in organic matter associated with the mineral fraction (mOM) and Potential carbon saturation (Sat-pot).

Coefficients	Estimate	Asymptotic Std. Error	z value	Pr(>|z|)	Impact Direct	Impact p-value
			C in organic matter associated with the mineral fraction (mOM)			
			0–20 cm			
(Intercept)	−0.81	1.41	−0.57	0.57		
AKln	−278.9	137.1	−2.03	0.041	−283.7	0.061
AGbs	1283.4	364.8	3.52	**0.0004**	**1305.4**	**0.0007**
AGt	164.7	38.4	4.29	**1.75E^{-05}**	**167.6**	**8.94E^{-06}**
AHem	183.2	85.9	2.13	0.032	186.3	0.028
			80–100 cm			
(Intercept)	−1.71	1.78	−0.95	0.34		
AGbs	720.1	234.1	3.07	**0.002**	**739.8**	**0.003**
AGt	66.6	22.9	2.91	0.003	68.4	**0.009**
AHem	188.4	57.8	3.26	**0.001**	**193.6**	**0.0009**
			Potential carbon saturation (mg g^{-1}) (Sat-pot)			
			0–20 cm			
(Intercept)	−0.46	1.3	−0.35	0.72		
AKln	616.6	121.6	5.07	**3.95E^{-07}**	**621.6**	**4.95E^{-07}**
AHem	824.2	65.9	12.5	**2.22E^{-16}**	**830.9**	**2.22E^{-16}**
			80–100 cm			
(Intercept)	−3.03	1.15	−2.61	0.009		
AKln	716.4	110.8	6.47	**9.98E^{-11}**	**729.5**	**0.0002**
AGbs	886.4	385.4	2.30	0.021	902.7	0.035
AHem	346.4	78.4	4.42	**1.004E^{-05}**	**352.8**	**6.36E^{-05}**

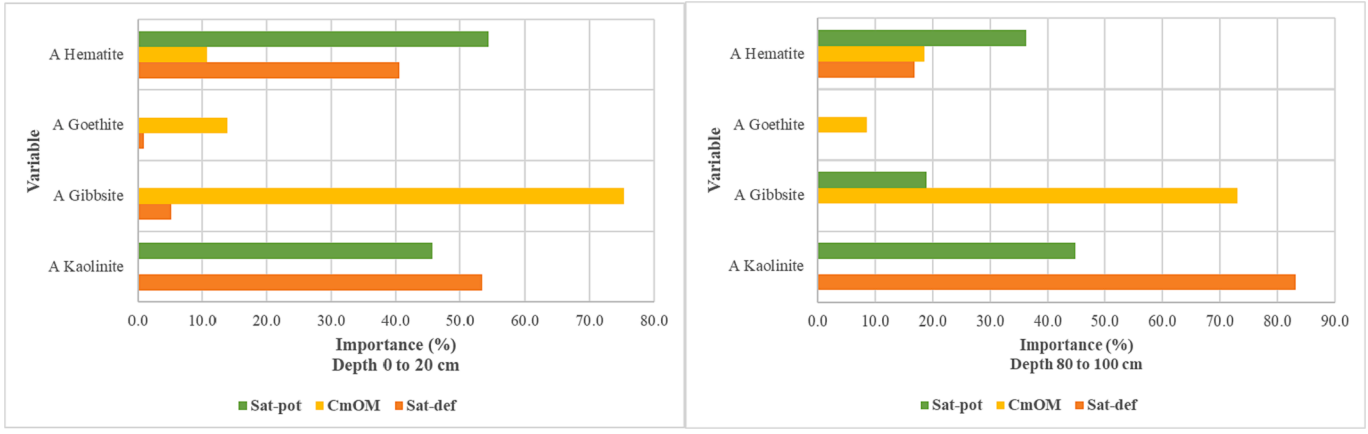

Fig. 5. Importance of the explanatory variables of the SARAR spatial regression model for depths 0 to 20 cm and 8 to 100 cm for the potential carbon saturation deficit or carbon sequestration potential (sat-def), C in organic matter associated with the mineral fraction (CmOM) and Potential carbon saturation (sat-pot).

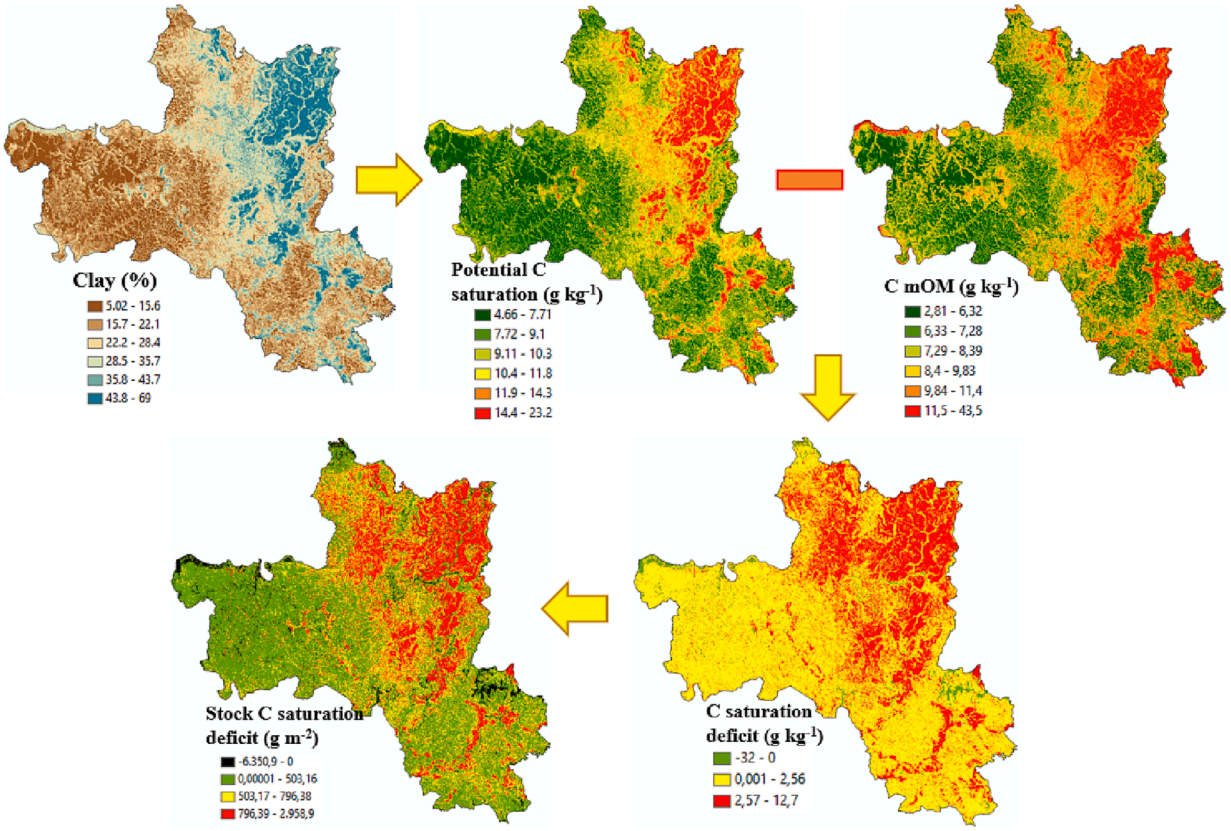

Fig. 6. Carbon saturation potential, C in organic matter associated with the mineral fraction (mOM), saturation deficit, and deficit stock associated with clay contents at soil depth of 0 to 20 cm.

equation by Feller and Beare (1997) for tropical soils was used, as it included samples of Brazilian clay soils with iron and aluminum oxyhydroxides, some located in our study area (Fig. 2):

$$C_{sat\text{-}pot} = 3.2 + 0.29 * \text{Particles} \leq 20\ \mu m\ (\%)\ (r = 0.95,\ p < 0.001)$$

In this study, the value of the percentage of fine soil particles (particles ≤ 20 μm (%)) was replaced by the percentage of clay. The silt fraction, both coarse (20–53 μm) and fine fraction (2–20 μm), was not used in this study, as it was reported that the silt fraction of highly weathered soils with high contents of kaolinite and iron and aluminum oxides store a small amount of carbon, representing about 4.8% of the total C content (Rodrigues et al., 2022). Fig. 2 shows the methodological sequence of the point modeling to determine the C sequestration potential and to generate an equation to predict this potential based on spectral information associated with the minerals of the clay fraction.

The determination of the C saturation deficit requires the actual concentration of C in the fine soil particles (<20 μm). For this, 35 representative soil samples were selected from the study area, based on the conditioned Latin hypercube sampling method, which corresponds to a stratified random sampling procedure where the selected samples follow multivariate characteristics according to the indicated covariables (Yang et al., 2020). Here, the Soil Synthetic Image (SYSI), soil type and variability in clay and C content were considered as covariates.

In these representative samples, fractionation was performed to quantify the C in particulate organic matter and the C in organic matter associated with the mineral fraction (mOM) (Cotrufo et al., 2019) following the methodology described by Jindaluang et al. (2013). The soil was dispersed using 5% sodium hexamethasphate solution and considering the low contribution of the coarse and fine silt fraction to the total carbon storage described by Rodrigues et al. (2022) the separation of sand and clay/silt faction was performed by 53 μm sieving. Subsequently, a linear regression model based on the total SOC content and mOM was developed to predict the C content of mOM in the remaining samples, with an R^2 fit of 0.98 (Fig. 3). Therefore, the C saturation deficit, corresponds to the expression:

$$C_{sat\text{-}def} = C_{satpot}\text{-}\ (0.8966 * SOC_{\ total} + 0.0773)$$

Subsequently, the carbon reserve or stock of this difference is calculated from this difference, using the Benites et al. (2007) equations:

$$SOC - stock\ =\ (SOC\ \times\ D\ \times\ BD)\ \times 10$$

Where: SOC-stock = Soil Organic Carbon Stock (g m^{-2}), SOC = Soil Organic Carbon content (g kg^{-1}), D = soil thickness (cm), BD = bulk density (g cm^{-3}). The bulk density is calculated from:

$$BD\left(g\ cm^{-3}\right) = 1.5688 - 0.0005 \times clay\ \left(g\ kg^{-1}\right) - 0.0090 \times SOC\ \left(g\ kg^{-1}\right)$$

2.2.2. *Spatial regression analysis*

As pointed out by Marschner et al. (2008), predictions of SOC storage potential require an understanding of the processes related to SOC sequestration and release. Several authors (Hassink, 1997; Yang et al., 2021; Kirsten et al., 2021), highlighted the importance of minerals associated with the clay fraction in C sequestration because they involve variable amounts of minerals that have an affinity with organic molecules, according to the interaction on their surfaces that favors the formation of organic-mineral complexes (Sollins et al., 1996, Von Lützow et al., 2006), reflecting in higher stability of SOC (De Mastro et al., 2020). Thus, this study focused on specifically demonstrating the response of variability in mineralogy on SOC sequestration potential; therefore, regression models were built to predict the theoretical potential SOC saturation deficit (Sat-def), potential C saturation (Sat-pot), and C in mineral-associated organic matter (CmOM), each as a function of the mineral contents that make up the clay fraction. According to

Table 5
Areas expressed in m^2 with high, medium and low potential saturation of COS according to historical land use, type of mineral and soil depth A) from 0 to 20 cm, B) from 40 to 60 cm, C) from 80 to 100 cm.

Depth	Mineral	C retention potential	Agriculture	Agriculture + Forest	Agriculture + Pasture	Agriculture + pasture + forest	Agriculture50 + forest	Agriculture50 + pasture	Forest	Forest + pasture	Forest50 + agriculture	forest50 + pasture	Pasture	Pasture50 + agriculture	Urban + road	Water
A	**Kaolinite**	Low	**52396.6**	465.6	262.7	23562.2	20265.8	38032.0	4393.6	1.6	7323.5	215.1	15.9	1842.2	12186.4	1802.7
		Medium	13677.1	42.0	146.2	6874.3	3763.8	29507.4	473.8	0.4	858.5	19.2	17.6	2106.3	1782.6	36.8
		High	**7360.7**	19.5	104.4	2856.0	1661.7	**19954.7**	201.0	0.0	325.6	4.5	16.4	1649.2	648.8	15.6
	Goethite	Low	73434.3	527.1	513.4	33292.5	25691.2	87493.8	5068.4	2.0	8507.6	238.7	50.0	5597.7	14617.8	1855.1
		Medium	0.0	0.0	0.0	0.0	0.0	0.0	0.0	0.0	0.0	0.0	0.0	0.0	0.0	0.0
		High	0.1	0.0	0.0	0.0	0.0	0.2	0.0	0.0	0.0	0.0	0.0	0.0	0.0	0.0
	Hematite	Low	66288.9	485.9	460.3	30888.7	23123.2	77702.7	4761.1	2.0	8002.5	232.5	43.2	4990.3	14130.4	1728.4
		Medium	3688.8	17.2	37.8	1507.7	1270.6	6256.7	174.5	0.1	275.2	3.5	5.7	495.5	284.7	29.9
		High	**3456.6**	24.0	15.2	896.1	**1297.4**	**3534.7**	132.9	0.0	229.9	2.7	1.1	111.9	202.7	96.8
B	**Kaolinite**	Low	71.4	12.8	6.2	163.2	81.5	133.5	15.0	0.0	28.6	0.9	0.0	9.5	123.6	107.7
		Medium	48898.5	435.4	341.2	25196.8	19562.4	50230.5	3977.6	1.7	6771.1	203.7	33.1	3593.9	10811.2	1666.4
		High	**24464.5**	78.9	166.0	7932.5	6047.4	**37130.0**	1075.8	0.3	1707.9	34.1	16.9	1994.2	3683.0	80.9
	Goethite	Low	40753.6	385.4	131.9	11137.0	14632.5	17110.1	2298.7	0.5	3909.2	112.9	0.7	224.8	9804.2	1749.9
		Medium	29688.4	141.0	342.2	21566.7	10708.3	**61886.3**	2769.4	1.6	4591.3	125.9	45.4	4814.1	4653.6	105.2
		High	**2992.3**	0.6	39.3	588.8	350.4	**8497.7**	0.3	0.0	7.1	0.0	3.8	558.7	160.0	0.0
	Hematite	Low	28685.1	348.7	144.8	13647.5	13272.1	19183.1	2379.2	0.6	4280.7	130.3	3.0	589.5	8785.2	1678.6
		Medium	23448.0	112.6	186.1	11982.5	7155.1	35365.3	1624.2	1.2	2648.0	70.4	23.4	2413.4	3562.1	120.4
		High	**21301.2**	65.7	182.5	7662.5	5264.0	**32945.6**	1065.0	0.2	1578.8	38.0	23.6	2594.8	2270.6	56.1
C	**Kaolinite**	Low	5.2	0.0	0.0	1.5	1.4	0.9	0.0	0.0	0.3	0.1	0.0	0.2	1.4	0.0
		Medium	50559.7	354.1	386.9	24990.2	18462.5	57869.0	4162.6	1.7	6751.2	199.0	42.3	4554.3	9986.5	1302.4
		High	**22869.4**	173.0	126.5	8300.8	7227.3	**29624.2**	905.9	0.3	1756.0	39.7	7.7	1043.2	4629.9	552.7
	Goethite	Low	16045.7	38.5	22.1	1323.4	4608.5	3656.2	96.6	0.0	209.0	5.9	0.2	52.1	2363.4	115.8
		Medium	33551.0	431.8	228.7	18888.6	14494.6	29235.3	3986.0	1.3	6420.1	183.0	9.5	1522.5	10177.2	1706.4
		High	23837.6	56.7	262.6	13080.4	6588.1	54602.6	985.9	0.7	1878.5	49.9	40.3	4023.0	2077.2	32.9
	Hematite	Low	3983.1	89.4	42.0	3303.2	2218.1	3529.6	572.7	0.2	1152.4	32.1	1.5	267.2	1649.2	613.1
		Medium	40247.3	294.0	374.5	24427.0	14854.8	62214.4	3759.0	1.6	6058.4	179.0	43.0	4681.5	9522.6	818.3
		High	**29204.0**	143.7	96.9	5562.3	8618.3	**21750.1**	736.7	0.2	1296.8	27.7	5.5	649.0	3446.0	423.6

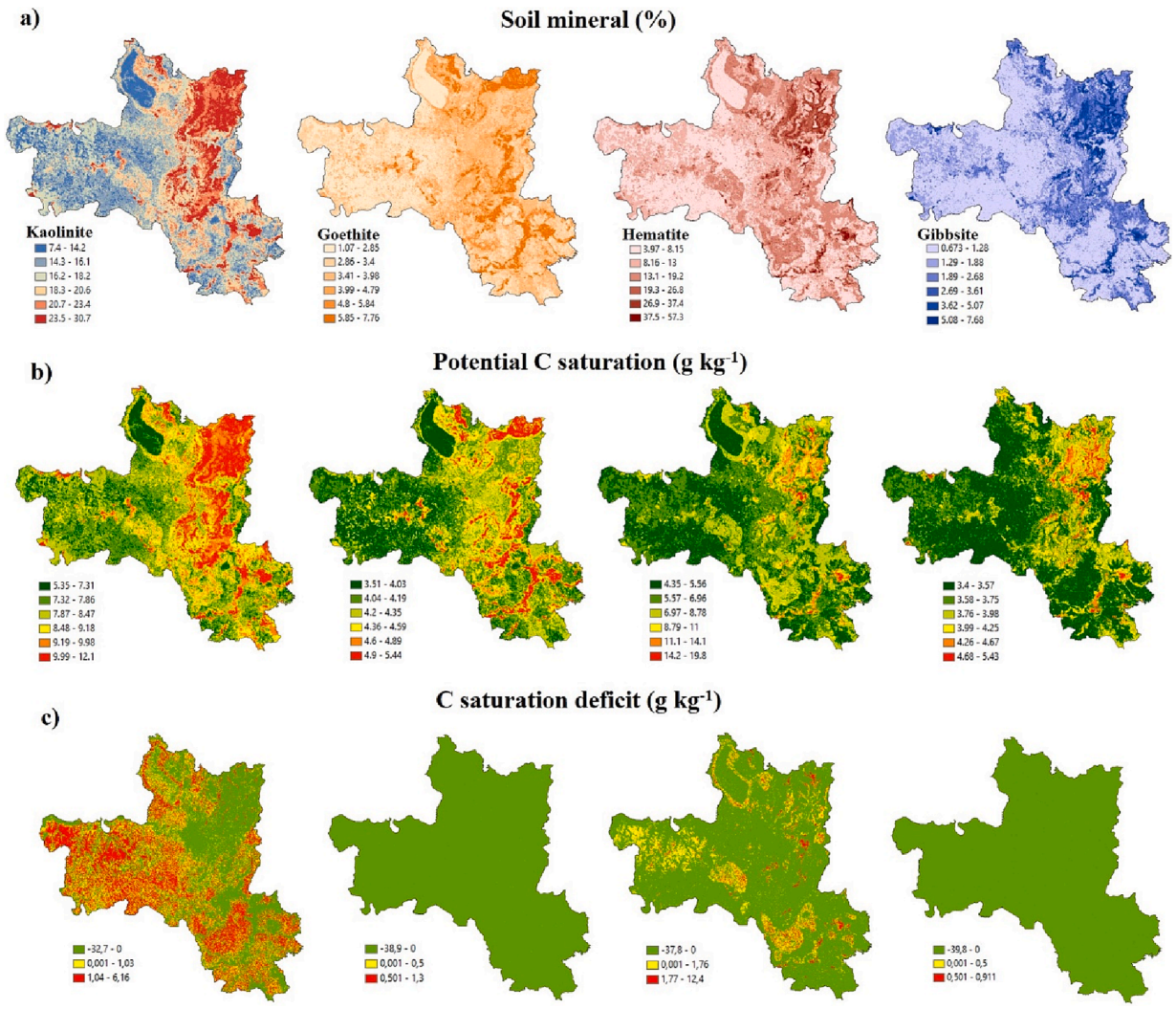

Fig. 7. Percentage of kaolinite, goethite, hematite, and gibbsite minerals (a), carbon saturation potential (b) and saturation deficit (c) for 0 to 20 cm.

Okunlola et al. (2021), the presence and quantity of a specific mineral content depend on the spatial location. Therefore, it was necessary to perform a regression analysis considering the geographic coordinates of the samples and the spatial dependence of soil variability (Webster and Oliver, 2007), so a weight matrix associated to all neighbors was generated.

The spatial regression analysis considered as dependent variables the potential SOC saturation deficit or potential SOC sequestration and potential C saturation (Sat-pot), calculated from the equation of Feller and Beller (1997) and the C in mineral-associated organic matter (CmOM) determined in the laboratory, as explanatory variables were considered the relative abundance of soil minerals represented by their infrared spectral amplitudes (calculated from diffuse reflectance spectroscopy data (Vis-NIR-SWIR)). The mineral amplitudes correspond to the difference between maxima and minima of the Savitzky-Golay second derivative curves obtained from the Kubelka-Munk absorption curves of the original spectra. These amplitudes were obtained from the study of Mendes et al. (2020), in which the bands associated with goethite (Gt, 422/450 nm), hematite (Hem, 535/575 nm), gibbsite (Gbs, 2265/2285 nm) and kaolinite (Kln, 1415/2205 nm) are defined. A data set of 1248 samples was taken for the 0 to 20 cm depth and 833 for the 80 to 100 cm depth.

Spatial regression models, such as spatial autocorrelation models (SAC; referred to in the literature as SARAR), spatially lagged models (SLM) and spatial error model (SEM and SDEM) were fitted to predict the potential SOC sequestration spatially (Elhorts, 2014). SARAR is a double autoregressive model that includes the autoregressive component of the response and the residuals, allowing to explain the spatial dependence of the residuals.

The models are expressed in the following equation:

$$Y = \lambda WY + \alpha\iota_n + X\beta + u; |u| < 1$$
$$u = \rho Wu + \varepsilon|\rho| < 1$$

Where, Y Where, Y represents the potential saturation deficit of SOC (Sat-def) or potential saturation of C (Sat-pot) or the CmOM, X represents the matrix of explanatory variables associated with the amplitude of minerals, W corresponds to the matrix of weights in relation to the distances of the nearest neighbor centroids in the polygons generated by tessellation of the soil sampling points, λ represents the spatial autoregressive coefficient, ρ the spatial autocorrelation coefficient, α corresponds to the intercept, β represents the parameters linked to the explanatory variables, u is associated with the vector of residuals with spatial dependence and ε $N(0, \sigma^2 I)$, where I is an identity matrix.

The choice of the model that best explains the statistical relationship of the experimental data was based on the lowest value of the Akaike information criterion (AIC) and on the fulfilment of the assumption of independence of the residuals based on the Moran Index Test (MIT), with the matrix of weights of all neighbors (Liu and Chen, 2021), where the p-value of the test must be greater than 0.05. In the case that more than one model satisfied the above assumptions, the highest correlation

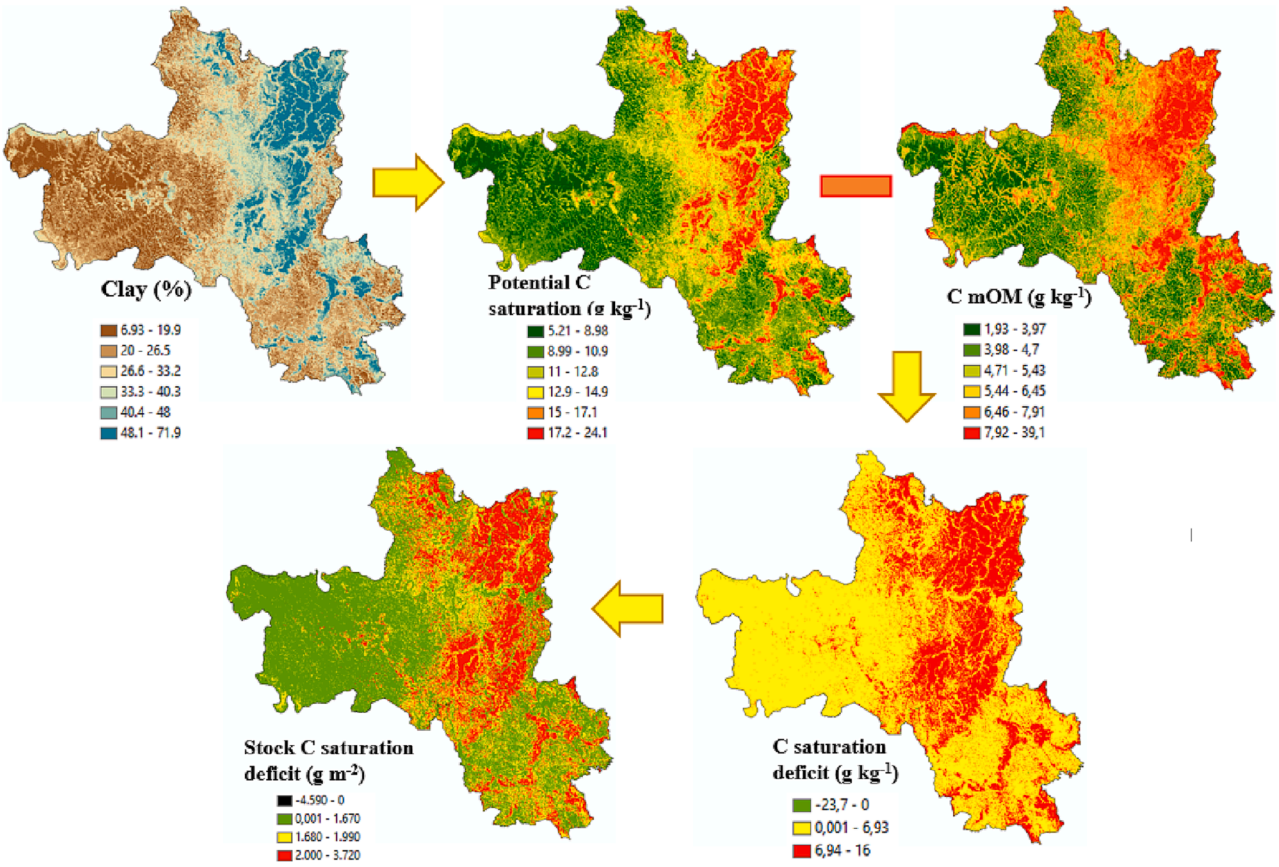

Fig. 8. Carbon saturation potential, C in organic matter associated with the mineral fraction (mOM), saturation deficit and deficit stock associated with clay contents at soil depth of 40 to 60 cm.

(r) between the observed values of response Y and the values estimated by the model was used as a criterion (Hoge et al., 2018).

Once the spatial regression model has been selected, it is important to evaluate and interpret the impact of the explanatory variables to determine the most important ones, however, in some spatial regression models, such as the autoregressive ones, it is not possible to perform this interpretation directly with the coefficients of the model as it is evaluated in classical regression models, therefore, according to Elhorst (2014), strategies are proposed for the estimation and interpretation of these coefficients, dividing them into direct, indirect and total impacts, which are obtained from the *impacts* function of the *spatialreg* library of R (Mendez, 2020). For the present study, the direct impacts are analyzed and the relative importance of each explanatory variable is calculated according to the total impacts.

2.3. Spatialization of carbon sequestration potential

The carbon sequestration potential of the clay fraction was spatialized by applying the equations described in the point modeling on the SOC and clay predicted maps for the different depths, as described in Fig. 4.

For SOC and clay mapping, covariables (predictors) associated with relief and a Synthetic Soil Image (SYSI) were used. The relief attributes included elevation, slope, aspect, curvatures, valleys, hills, orientation, and topographic wetness index as described by Carvalho et al. (2019) and Sabetizade et al. (2021). The terrain variables were from a digital elevation model (DEM) of the Radar Topography Mission – SRTM (USGS, 2018), at 30 m spatial resolution. The SYSI in turn corresponds to a mosaic of the bare soil surfaces obtained from the Landsat images collection from 1984 to 2020. The SYSI images contain six bands in the Vis-NIR-SWIR spectral range (blue, green, red, NIR, SWIR1 and SWIR2) and were obtained by applying the Geospatial Soil Sensing System (GEOS3), developed by Dematte et al. (2018).

The Random Forest (RF) algorithm was chosen for spatial prediction, as it was reported as the best performing predictive algorithm in SOC mapping (Khaledian and Miller, 2020, Zeraatpisheh et al., 2020, Lamichhane et al., 2019; Padarian et al., 2020). RF is a nonparametric model that performs classification and regression of sets through the construction of several decision trees in the training stage, where each tree is generated by a random vector (Breiman, 2001). The subdivisions within each tree are determined based on predictor variables chosen randomly from the set of variables (Coelho et al., 2020). Its strength is based on bootstrapping randomization of data and random input selection (Sothe et al., 2022) with replacement of the original data and internal validation with data not used in the bootstrap procedure (Khaledian and Miller, 2020, Zeraatpisheh et al., 2020). The samples ($n = 2354$) were randomly divided into 70% and 30% for calibration and validation, respectively. The adjusted coefficient of determination (R^2) was used as a model evaluation metric.

For the spatialization of the C sequestration potential of each of the minerals that compose the clay fraction (goethite, hematite, gibbsite and kaolinite), we used the mineral maps elaborated by Mendes et al. (2021), which were obtained by digital soil mapping, using diffuse reflectance spectroscopy (Vis-NIR-SWIR) to estimate mineral abundance at specific locations and environmental covariates for spatialization. As for the clay fraction, the equations described in the point model were applied using map algebra, where "Particles $\leq$ 20 μm (%)" was replaced by the abundance map of each mineral at different depths, leaving fixed the predicted SOC maps for the different depths. According to Sothe et al. (2022) in the use of machine learning models for SOC prediction it is possible to use the same model keeping some covariates fixed to identify the influence of the variable of interest in the SOC prediction.

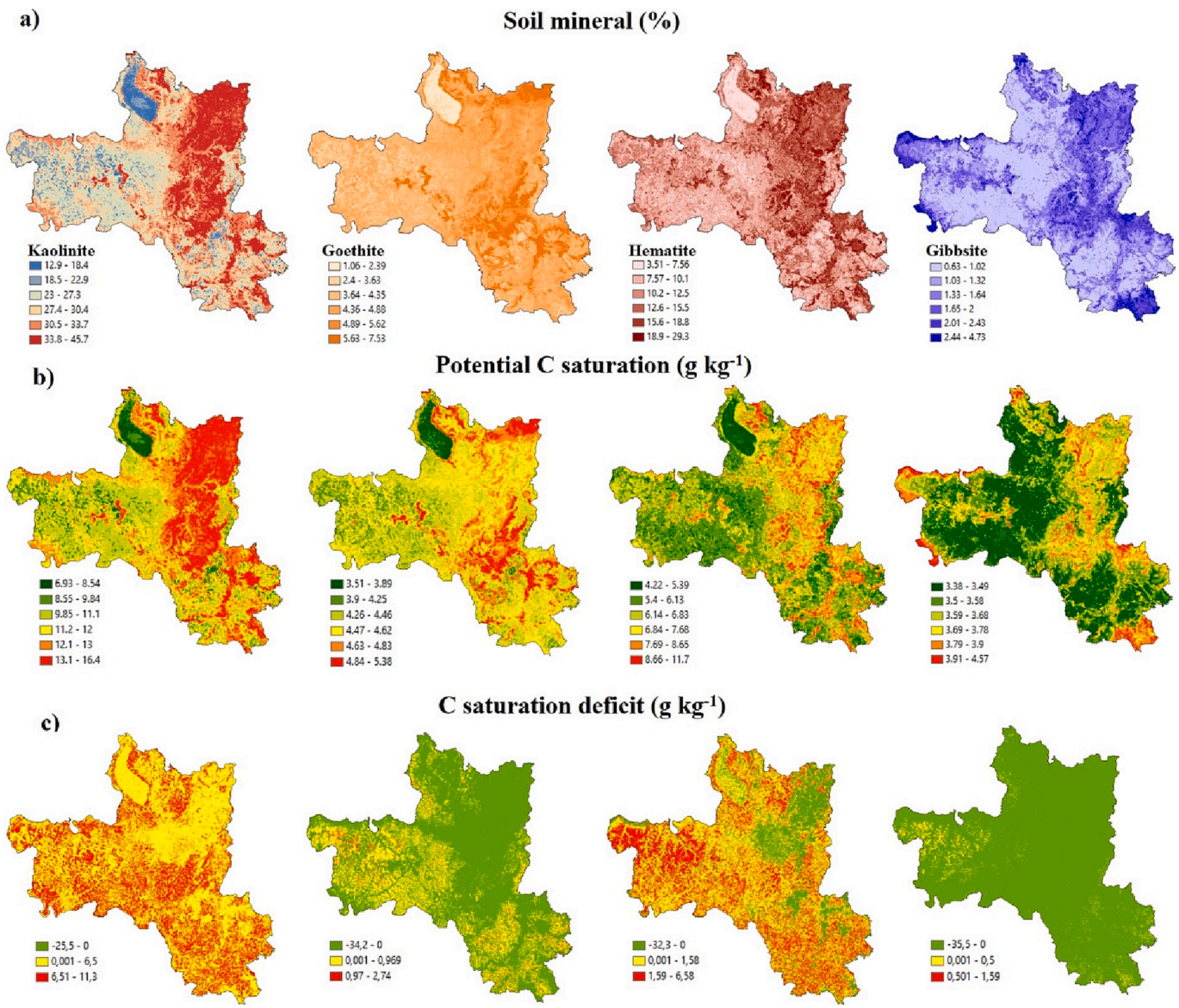

Fig. 9. Percentage of kaolinite, goethite, hematite, and gibbsite minerals (a), carbon saturation potential (b) and saturation deficit (c) for 40 to 60 cm.

Such spatialization will allow us to observe a spatial approximation of the individual contribution of the minerals that compose the clay fraction in the C sequestration potential, and together with the predictive model of this potential obtained from the spatial regression, will help to understand the dynamics of the potential of the mineralogy of the clay fraction to sequester new carbon.

3. Results

3.1. Point modeling of soil carbon sequestration potential

For the selection of the best fit models of the relationship between the response associated with the carbon sequestration potential or potential saturation deficit of SOC (Sat-def), potential saturation of C (Sat-pot) and CmOM with the explanatory variables related to mineral amplitude, the pure spatial autoregressive regression models (PAR), the spatial lag model (SLM), the spatial error (SEM), the spatial double autoregressive model (SARAR) and the spatial Durbin error (SDEM) were used were used, however the latter was excluded from Sat-pot and CmOM because a fit was not achieved (Tables 1 and 2).

Sat-def = potential carbon saturation deficit or carbon sequestration potential. A = amplitude of the different minerals AKln (kaolinite), AGt (goethite), AHem (hematite), AGbs (gibbsite).

Where A = amplitude of the different minerals AKln (kaolinite), AGt (goethite), AHem (hematite), AGbs (gibbsite).

Based on the MIT evaluation (Tables 1 and 2), only the SARAR model, for each of the dependent variables, satisfied the criteria. Based on AIC and r, the SARAR model also performed best in all three models for the depth of 0–20 cm (Sat-def: AIC = 6692 y r = 0,56; CmOM: AIC = 6659 y r = 0.60; Sat-pot: AIC = 6587 y r = 0.76) and 80–100 cm (Sat-def: AIC = 4429 y r = 0,66; CmOM: AIC = 3734 y r = 0.70; Sat-pot: AIC = 4481 y r = 0.66). For 0–20 cm, the SARAR model of carbon sequestration potential (Sat-def) includes all minerals, whereas, for the latter depth, it includes only kaolinite and hematite. CmOM is also explained by all minerals at the first depth, and the importance of kaolinite was lost in the last layer. On the contrary, Sat-pot at the first depth was only explained by kaolinite and hematite, and at the last depth kaolinite, gibbsite and hematite were considered.

Where A = amplitude of the different minerals AKln (kaolinite), AGt (goethite), AHem (hematite), AGbs (gibbsite). Pr (>IzI) is related to the significance of each variable in the model, with lower values highlighting greater importance.

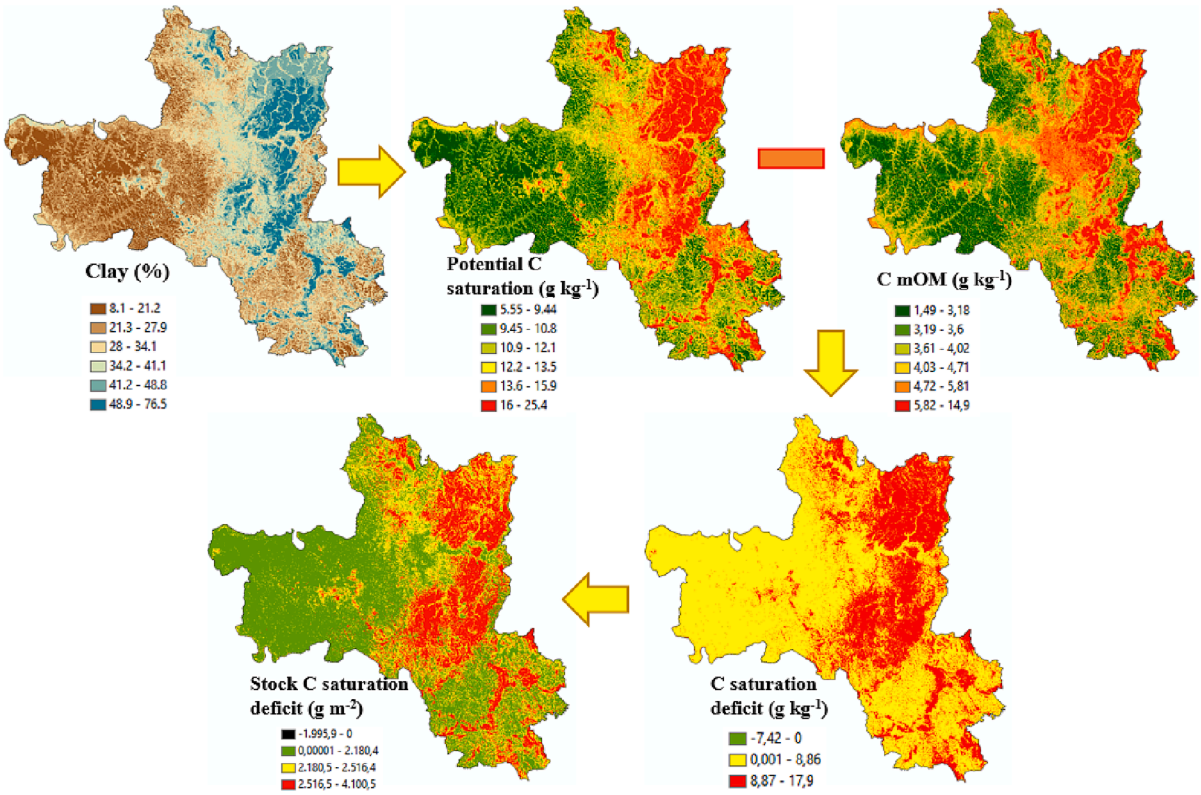

Fig. 10. Carbon saturation potential, C in organic matter associated with the mineral fraction (mOM), saturation deficit and deficit stock associated with clay contents at a soil depth of 80 to 100 cm.

Satdef = potential carbon saturation deficit or carbon sequestration potential. A = amplitude of the different minerals AKln (kaolinite), AGt (goethite), AHem (hematite), AGbs (gibbsite). Pr (>IzI) is related to the significance of each variable in the model, with lower values highlighting greater importance.

The models for each depth described in the tables 2 and 3 can be expressed from the matrix point of view as shown in the following equations:

1) For depth from 0 to 20 cm:

$$\begin{aligned}\text{Csat} - \text{def} &= 0.87Wy - 0.64 + 840AKln - 1264AGbs - 164AGt \\ &+ 612AHem + u; u \\ &= 0.66Wu + \varepsilon\end{aligned}$$

$$\begin{aligned}\text{C}\,mOM &= 0.88Wy - 0.81 - 278.9AKln + 1283.4AGbs + 164.7AGt \\ &+ 183.2AHem + u; u \\ &= 0.88Wu + \varepsilon\end{aligned}$$

$$\begin{aligned}\text{C}\,SatPot &= 0.89Wy - 0.46 + 616.6AKln + 824.2AHem + u; \\ u &= 0.71Wu + \varepsilon\end{aligned}$$

2) For depth from 80 to 100 cm:

$$\begin{aligned}\text{Csat} - \text{def} &= 0.82Wy - 1.66 + 600AKln + 127AHem + u; \\ u &= 0.85Wu + \varepsilon\end{aligned}$$

$$\begin{aligned}\text{C}\,mOM &= 0.94Wy - 1.71 + 720.1AGbs + 66.6AGt + 188.4AHem + u; \\ u &= 0.92Wu + \varepsilon\end{aligned}$$

$$\begin{aligned}\text{C}\,SatPot &= 0.86Wy - 3.03 + 716.4AKln + 886.4AGbs + 346.4AHem + u; \\ u &= 0.86Wu + \varepsilon\end{aligned}$$

Where, Sat-def = potential carbon saturation deficit or carbon sequestration potential, CmOM = C in organic matter associated with the mineral fraction, Sat-pot = Potential carbon saturation, A = amplitude of the different minerals AKln (kaolinite), AGt (goethite), AHem (hematite), AGbs (gibbsite), W corresponds to the matrix of weights, u is associated with the vector of residuals with spatial dependence and $\varepsilon\ N(0, \sigma^2 I)$, where I is an identity matrix.

The spatial modeling results show that the carbon sequestration potential (sat-def) for 0–20 cm depth could be explained by the relative contents of kaolinite, gibbsite, goethite and hematite (Table 3). Where kaolinite and hematite had the largest direct positive impact. On the contrary, a direct but negative impact was observed for goethite and gibbsite, which could indicate that an increase in the concentration of these minerals reduces the C sequestration potential of the soil, however these minerals have the highest affinity for organic molecules (Kaiser and Zech, 2000; Dos Reis et al., 2014), so they tend to saturate first compared to kaolinite and hematite, and stabilize more efficiently the sequestered C (Kalbitz et al., 2005; Dos Reis et al., 2014), in that sense, such negative impacts could then be translated as the higher concentration of these minerals, the greater stabilization of organic molecules may occur, that is, higher current COS content and lower potential to sequester new carbon. This explains the results of the model for potential C saturation (sat-pot, Table 4), corresponding to the theoretical maximum of SOC, which in the 0–20 cm depth was only explained by kaolinite and hematite, indicating that it is these minerals that have the potential to sequester new carbon.

It is also important to highlight that the CmOM model for the 0 to 20 cm depth (Table 4) shows greater importance in gibbsite and goethite (Fig. 5), due to the potential for stabilization of organic molecules presented by these minerals, which corroborates that these are the ones who contribute most to the current carbon, and contrary to the Sat-def model (Table 3), the negative impacts were presented in kaolinite, since, as mentioned above, the carbon associated with this mineral is related to the potential for sequestering new carbon. On the other hand, the carbon sequestration potential (sat-def) for the 80 to 100 cm depth (Table 3) was mainly explained by the contents of kaolinite and

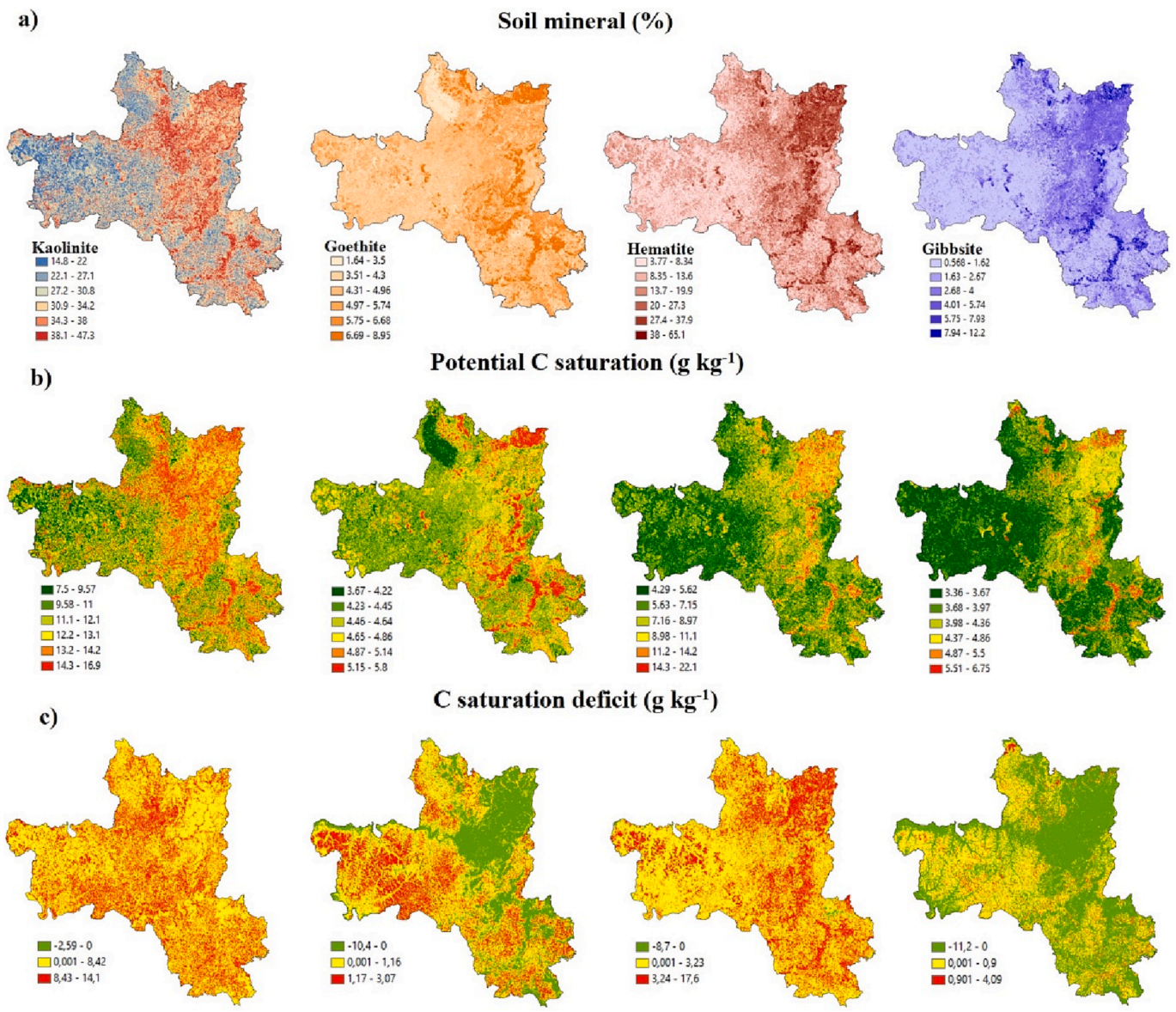

Fig. 11. Percentage of kaolinite, goethite, hematite, and gibbsite minerals (a), carbon saturation potential (b) and saturation deficit (c) for 80 to 100 cm.

hematite, with the greatest impact of kaolinite (Fig. 5). CmOM at this depth (Table 4) was mainly explained by gibbsite, goethite and hematite, with greater impact of gibbsite and hematite (Fig. 5). On the contrary, Sat-pot was explained by kaolinite, gibbsite and hematite with higher impact of kaolinite and hematite. It is important to highlight the importance of hematite in the carbon sequestration and stabilization cycle at the two depths, since in all three models it is a variable of high importance (Fig. 5). According to Georgiou et al. (2022) increasing mineral-associated C is key to long-lasting C sequestration, and for the soils of the study region hematite responds to these additional spaces to sequester and stabilize new C along the soil profile.

In general, the participation of goethite and gibbsite in explaining the C sequestration potential (sat-def) was low in the 0 to 20 cm depth and null in the 80 to 100 cm depth (Fig. 5), with greater importance of kaolinite compared to hematite, whose difference was not so marked for the 0 to 20 cm depth.

3.2. Carbon sequestration potential mapping

Carbon and clay maps were obtained for the different depths using DSM with R^2 of 0.6 and 0.7, respectively. Areas with higher clay content had a higher carbon sequestration potential (areas in red), that is, the minerals that compose this fraction had the potential to retain more carbon, and these were related to agricultural areas (Figs. 6 and 13, Table 5). On the contrary, areas with more than 15 years under the same land use, such as pastures and forests (Figs. 6 and 13, Table 5), had less potential for additional carbon sequestration.

When evaluating the individual contribution of each mineral (Fig. 7), it was observed that the zones with the highest C sequestration potential in Fig. 6 corresponded to areas that were saturated, highlighting the importance of the individual analysis of the minerals that make up the clay fraction, because evidently not all of them have the potential to sequester new carbon, being kaolinite and hematite those that still have space to store new carbon in the 0 to 20 cm depth, which was consistent with the result of the spatial regression models in Tables 3 and 4 elated to Sat-def and Sat-pot. Spatially, a high C sequestration potential was evidenced for kaolinite in the areas related to pasture and agricultural mosaics with more than 15 years (Fig. 13, Table 5), and the agricultural zone presented a low to null C sequestration potential (Fig. 7, Fig. 13). For gibbsite and goethite, zero sequestration potential was observed, indicating C saturation since the major contribution of these minerals translates into the current C associated with the mineral fraction

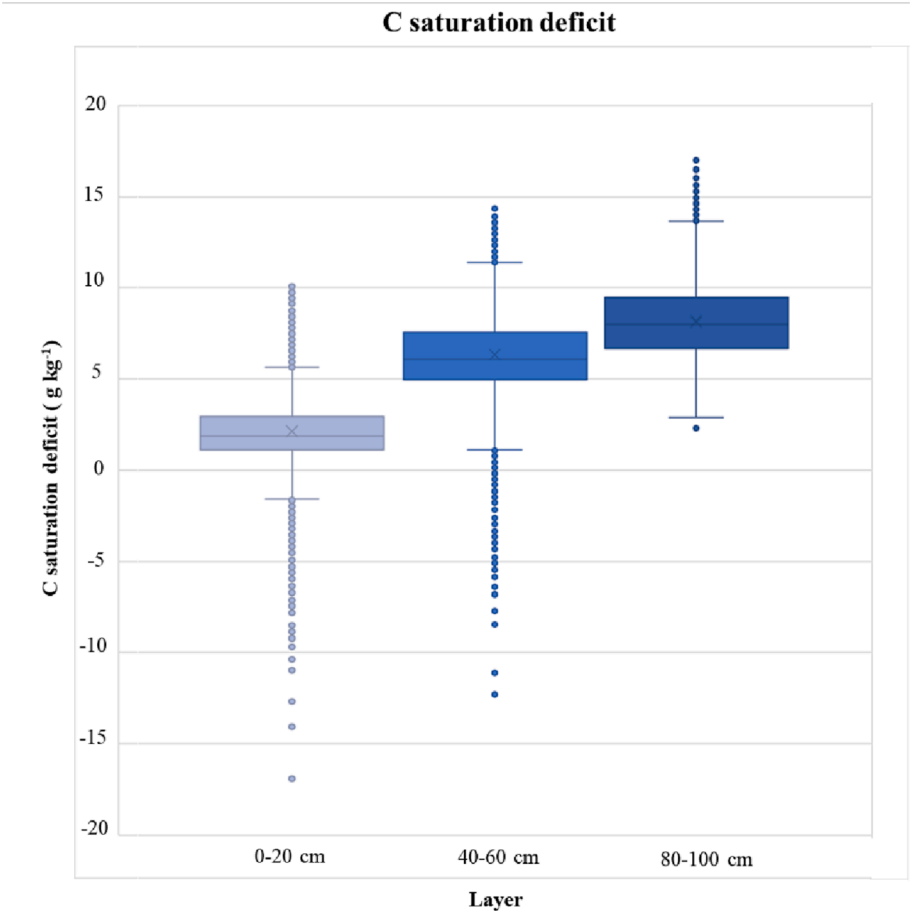

Fig. 12. Variation of the content of the potential C saturation deficit or C sequestration potential, at different soil depths.

(CmOM), confirming their low importance in the Sat-def spatial regression model (Fig. 5). On the other hand, areas dominated by hematite had a medium to high sequestration potential. Areas under agriculture and agricultural mosaics with pastures and forests showed the highest potential for carbon sequestration by hematite.

For the 40–60 cm and 80–100 cm depths, an increase in carbon sequestration potential was observed compared to the 0–20 cm depth (Figs. 8, 10 and 12). Specifically, the increase in potential in relation to the first depth was observed in the agricultural zones, from the north and southwest of the study area, with a considerable improvement in the zones that had mixed pasture and cropping (Fig. 13, Table 5).

Higher mineral contents were observed in the deeper layers (Figs. 9 and 11), especially kaolinite. However, the contents of other minerals showed a reduction at 40–60 cm and a considerable increase at 80–100 cm depth, which was reflected in an increase in C sequestration potential. It should be noted that even with the reduction of iron and aluminum oxide minerals contents at depth 40–60 cm (Fig. 9), a considerable improvement in the carbon sequestration potential of hematite and kaolinite were observed. A slight improvement in the potential of gibbsite and goethite was also observed, where gibbsite maintains a low potential in most of the area, with a slight improvement in the proximity of pasture, forest and cropping mosaics. The increase in C sequestration potential for goethite was observed in areas with crop and pasture mosaics. For hematite, low C sequestration potential was maintained in the northeastern part of the study area, corresponding to areas with more than 15 years in agriculture (Fig. 13, Table 5).

For 80–100 cm, the results of Sothe et al. (2022) were confirmed, showing that the kaolinite and the iron and aluminum oxides were not fully saturated (Figs. 10 and 11). C sequestration potential was higher, observing an increase in the potential for hematite in the areas under agriculture, with an increase in hematite potential observed in the areas under agriculture, which at depths 40–60 cm still showed low sequestration potential. Similarly, an increase in the sequestration potential for goethite and gibbsite were observed in the areas with pasture and cropping mosaics, maintaining a low potential in the areas with agricultural use for more than 15 years (Fig. 13, Table 5). Statistically, the point modelling highlighted the importance of kaolinite and hematite in the carbon sequestration potential of this depth (Table 3), however, it did not consider this contribution of gibbsite and goethite.

In general, it was observed that as the depth increases, there is a greater potential for sequestration of new C (Fig. 12), because there is less current C content in the mineral fraction, as Georgiou et al. (2022) mention, the greater the depth, the greater the subsaturation of C associated with minerals, therefore it is possible to consider that there is a potential carbon pool that could be exploited with the inclusion of shrub and tree crops whose root system reaches deeper into the soil.

4. Discussion

According to Boddey et al. (2010), the analysis of carbon storage potential requires the evaluation of deeper soil layers because studies from 0 to 100 cm depth reveal 59% more storage in relation to a study from 0 to 30 cm. That is, the inclusion of depth allows adequate prediction of SOC concentration (Sothe et al., 2022), since at shallower depths the mineral particles are more saturated with SOC. Therefore, depth allows for improved analysis of SOC storage potential (Hobley et al., 2015). This was confirmed in the present study, where with increasing depth a higher carbon sequestration potential was observed (Fig. 12), due to lower carbon saturation in clay fraction minerals such as kaolinite, hematite, goethite and gibbsite (Figs. 7, 9 and 11) and to the

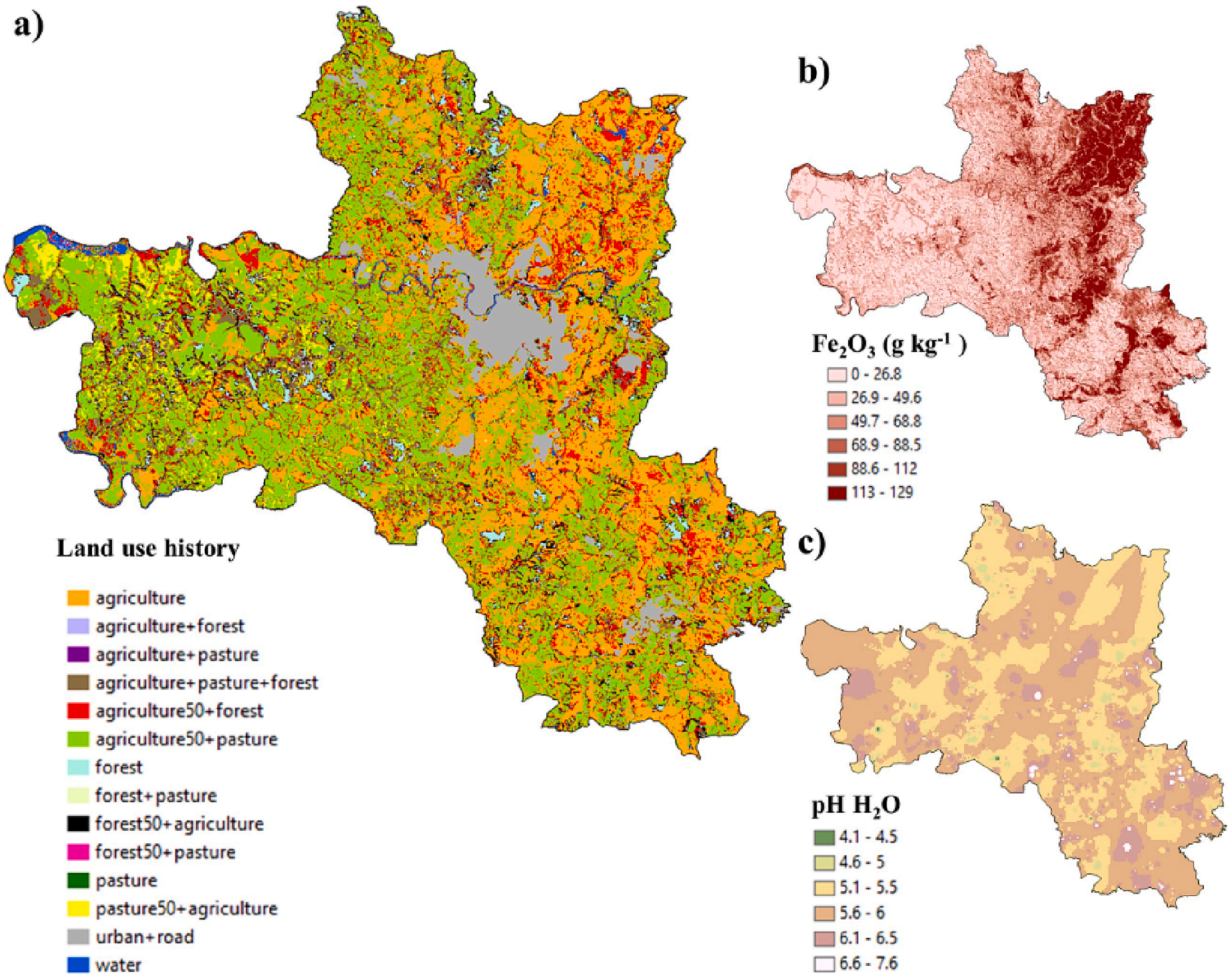

Fig. 13. Additional variables, Land use history (1985–2015) based on Tayebi et al. (2021) (a), iron oxide (F_2O_3) (b) and pH in water (c).

increase in the content of these minerals with depth, as they are more commonly found in highly weathered soils, with greater homogeneity in depth (Berg and Oliveira, 2000) and according to Georgiou et al. (2022) the maximum C content associated with minerals depends on the amount and type of mineral.

Ingram and Fernandes (2001), Weil and Brady (2016), indicated the importance of clay mineralogy on the potential of a soil to store organic carbon, especially in the deeper layers (Gray et al., 2015, Wiesmeier et al., 2011). In the present study, the spatial regression models showed a clear difference in the minerals contributing to carbon sequestration potential at depth 0 to 20 and 80 to 100 cm (Table 2), with low contribution of gibbsite and goethite at the deeper depth. However, in Figs. 9 and 11, the contribution of goethite and gibbsite in this overall contribution of new carbon sequestration that is not seen in the statistical model was observed.

Interpreting the individual contribution of the carbon sequestration potential of the clay fraction minerals is difficult due to their coexistence (Kirsten et al., 2021). Georgiou et al. (2022) points out the importance of generating mathematical models that allow inferring the C associated with the mineral fraction, however, their study was based on the limit line analysis where the determination of the C saturation potential is based on the highest C stocks and C contents in soils with presence of 2:1 clays and poorly crystalline minerals, which theoretically have higher capacity to stabilize C. For the present study this theoretical maximum limit was calculated as the potential C saturation based on the equation of Feller and Beare (1997) and spatial regression models were used to explain this potential C saturation (Sat-pot), the C associated with the mineral fraction (CmOM) and the potential for sequestration of new C (Sat-def) as a function of the relative abundance of the minerals that compose the clay fraction, finding the best fits with the SARAR double autoregressive spatial regression model, highlighting that the main contributing minerals in the C sequestration potential correspond to kaolinite and hematite (Table 3), with a low contribution of goethite and gibbsite in the 0 to 20 cm depth (Fig. 5). These minerals have direct impacts that indicate that a reduction in their concentration could reduce the C sequestration potential of the study area, since they are the minerals that contribute most to C stabilization and to the CmOM content.

According to Schaefer et al. (2008), the clay fraction of Brazilian soils is dominated by kaolinite and low crystallinity Fe and Al oxides, typically corresponding to gibbsite, hematite, goethite and maghemite (Kämpf and Curi, 2003). This low crystallinity of these iron oxides in Brazilian soils translates into more effective OM stability than crystalline Fe oxides or oxyhydroxides (Schaefer et al., 2008), because they exhibit electrostatic attractions and ionic bonds between the hydroxyl groups of the oxides and the carboxyl or hydroxyl groups of the OM (Duiker et al., 2003, De Mastro et al., 2020). In our study area, the presence of parental material associated with basalt (Fig. 1) allows locating ferruginous minerals of low degree of crystallinity according to Tombácz et al. (2004) and Ashton et al. (2016). Such localization coincides with the concentration of iron oxides with higher affinity for the MO (Ashton et al., 2016), which highlights that the reduction of goethite and gibbsite contents affects the stabilized MO, since as observed in the CmOM model, these minerals account for approximately 90% of the importance in explaining the current C of the mineral fraction (Fig. 5).

According to Guzmán et al. (1994), goethite usually presents greater

affinity for OM because it presents a double network of octahedra, where Fe^{+3} occupies only half of the spaces (Bigham et al., 2002). It gives a greater specific surface area for this oxide, compared to hematite, which presents an occupation of Fe^{+3} in 66% of the oxygens, reducing its specific surface area (Bigham et al., 2002) considerably. Kaiser and Guggenberger (2000) indicated that goethite and gibbsite have a high density of reactive sorptive sites, allowing more effective organo-mineral interactions. Hematite has a denser structure and lower surface area compared to goethite, having lower reactivity of hydroxyl groups on its surface (Dos Reis et al., 2014). Therefore, carbon had affinity and preference for goethite (Figs. 7 and 9). Similarly, it was found that gibbsite also had higher carbon saturation potential.

A decrease in pH increases the positive charges of iron oxides, increasing OC sorption (Ashton et al., 2016). However, the high presence of kaolinite could generate an increase in the negative charges neutralizing the positive charges of the oxides. In turn, it could lead to a reduction of stabilized OC (Kirsten et al., 2021), which is evidenced in the greater carbon retention potential, being clear the role played by pH (Ashton et al., 2016), as it influences the surface charge and therefore the adsorption capacity of organic compounds (Saidy et al., 2013). The pH control of the protonation and deprotonation of hydroxyl groups (Wang *et al.*, 2020). For the study area, the more significant presence of kaolinite was related to a high hematite content, especially in the eastern region, where pH ranged from strongly acidic (5 to 5.5) to moderately acidic (5.6 to 6) (Fig. 13), which could also explain the high potential for carbon sequestration in these areas.

Land use type also influences SOC content due to differences in vegetation and C input. Agricultural and highly degraded soils have considerable potential to store additional SOC (Wiesmeier et al., 2013, Georgiou et al., 2022), as a marked depletion of SOC stocks is observed (Paustian et al., 1997, Lal, 2004, Smith, 2004, Follett et al., 2001, Padarian et al., 2022). Sothe et al. (2022), reported a higher concentration of SOC in crops than in grazing land. Areas with more than 15 years of agriculture had both the lowest and the highest carbon sequestration potential (Table 5), that is, minerals such as goethite and gibbsite at depth 0 to 20 cm present a low potential to sequester new carbon in the study area and at greater depth the low potential is concentrated in these areas with traditional agricultural use. On the other hand, at shallower depths, minerals such as hematite and kaolinite had a higher sequestration potential, being higher for kaolinite in areas of pasture and cropping mosaics, and higher for hematite in areas with cropping mosaics of pasture and forest. With increasing depth, unlike goethite and gibbsite, kaolinite and hematite had high carbon sequestration potential in areas with traditional agricultural use. In agricultural areas, management practices that favor sequestration are related to the promotion of organic inputs, conservation/minimum tillage, conversion of cropland to pasture, introduction of perennials, proper management of cultivated peatlands, and organic farming (Sauerbeck, 2001, Vleeshouwers and Verhagen, 2002, Freibauer et al., 2004, Lal, 2004, Johnson et al., 2007, Smith, 2012). Rabbi et al. (2015) and Ashton et al. (2016), reported that conversion of cropland to grassland could increase carbon sequestration, that coincides with the observed results.

Afforestation and pasture improvements could contribute with soil carbon storage increase (Zeraatpishe and Khormali, 2012, Nave et al., 2013). It has also been reported when conversion from forest to managed pasture and from cropland to pasture occurred (Poeplau and Don, 2013). The areas under exclusively forest use presents low sequestration potential and the minerals such as goethite were highly saturated. On the other hand, areas with cropping and pasture mosaics presents a medium potential for carbon sequestration. However, it was evident that as the depth increases, the carbon sequestration potential improves in the forest uses, especially in agriculture and forest mosaics. For Minasny et al. (2013), historical land use is a variable that influences the explanation of carbon concentrations in deeper soil layers. Land use change can favor carbon sequestration because it results in a variation of organic compounds reaching the soil and mechanization can reactivate the carbon cycle, where bacteria in the environment take advantage of the released carbon, however, there are residues of this microbial decomposition that can be retained by minerals (Kirsten et al., 2021).

Acosta-Martinez et al. (2004) concluded that continuous monoculture systems had a negative impact on soil function and sustainability. Cultivation and tillage reduce and change the distribution of SOC, while appropriate crop rotation can increase or maintain the quantity and quality of SOM, improving soil chemical and physical properties (Liu et al., 2006). Crop intensity or frequency affects SOC storage by modifying the amount of time the soil is supporting a crop, thereby increasing annual production and C input to the soil (Ogle et al., 2005). Areas with the same land use for more than 15 years were those with higher saturation of minerals, such as goethite and gibbsite (higher affinity for SOM), as well kaolinite and hematite (low affinity for SOM). However, it was clear that those areas with agriculture and pasture mosaics, and pasture and forest mosaics, had the greater potential to retain new carbon, and its potential increases with soil depth (Table 5).

These areas with higher retention potential due to mineralogy are key to promote CO_2 sequestration by agroforestry and silvopastoral systems, because as evidenced, it is important to exploit the potential of goethite and gibbsite at depth (Fig. 11, Table 5), since, as indicated by Georgiou et al. (2022), the deeper the soil minerals are, the less saturated they become. Additionally, crop rotation or cover crops to exploit the potential of the most superficial layers of the soil is also important. The results presented could contribute to climate change mitigation strategies, as described by Minasny et al. (2017), who pointed out that at the 21st Conference of the Parties to the United Nations Framework Convention on Climate Change in Paris (COP21) the strategy “4 per thousand soils for food security and climate” was unveiled. This strategy aims to increase global soil organic matter stocks by 4 per 1000 (or 0.4%) per year considering soil organic carbon sequestration as a possible solution to mitigate climate change by taking atmospheric CO_2 and converting it into long-lived soil carbon.

The land uses described correspond to a historical use analysis for a period of 30 years. The number 50 in the heading relates to the middle of the period under this use. The highlighted numbering indicates the largest areas with high, medium and low carbon saturation potential.

5. Conclusions

The C sequestration potential prediction models obtained in the present study confirm the importance of the minerals that compose the clay fraction in the C sequestration potential of the soil. The prediction of this potential was fitted to a spatial regression model SARAR (Spatial AutoRegressive-AutoRegressive model) for depths of 0 to 20 and 80 to 100 cm, where at a depth of 0 to 20 cm the sequestration potential is explained by the content of kaolinite, hematite, goethite and gibbsite, with kaolinite and hematite being the most important explanatory variables. On the other hand, goethite and gibbsite had a direct but negative impact, indicating that an increase in the concentration of these minerals reduces the potential for sequestration of new C, due to the affinity they have with organic molecules, so they tend to saturate reducing their potential to store new carbon, but translates into greater stability of organic molecules and higher current COS content. For the 80 to 100 cm depth, the prediction of carbon sequestration potential was explained by the content of kaolinite and hematite, with greater importance of kaolinite. Hematite is a mineral of importance in carbon sequestration and stabilization since it was a variable of high importance in explaining mineral-associated C (CmOM), potential C saturation (Sat-pot) and C sequestration potential (Sat-def) at different depths.

Soil carbon sequestration potential by mineralogy is strongly influenced by land use. Areas of pasture and crop on soils with high kaolinite and hematite content presented greater potential to sequester carbon. In addition, areas with lower pH and higher kaolinite and hematite content also have a high potential for carbon sequestration, which can be enhanced by land use change.

Gibbsite and goethite had a higher sorption power of organic molecules; therefore, they had a lower potential for sequestration of new carbon in areas with the same land use for more than 15 years, because they are the first minerals to become saturated, especially in the surface layers. However, their potential increases in cropping and pasture areas at greater depths because the concentration of SOM was lower. Soils at greater depths had the greatest potential for carbon sequestration and could be key for climate change mitigation strategies.

CRediT authorship contribution statement

Heidy Soledad Rodríguez-Albarracín: Conceptualization, Formal analysis, Methodology, Software, Visualization, Writing – original draft, Writing – review & editing. **José A.M. Demattê:** Conceptualization, Funding acquisition, Resources, Supervision, Validation, Writing – review & editing. **Nícolas Augusto Rosin:** Methodology, Software, Writing – review & editing. **Aquiles Enrique Darghan Contreras:** Methodology, Software, Writing – review & editing. **Nélida E.Q. Silvero:** Writing – review & editing. **Carlos Eduardo Pellegrino Cerri:** Visualization, Writing – review & editing. **Wanderson de Sousa Mendes:** Writing – review & editing. **Mahboobeh Tayebi:** Writing – review & editing.

Declaration of Competing Interest

The authors declare that they have no known competing financial interests or personal relationships that could have appeared to influence the work reported in this paper.

Data availability

The authors do not have permission to share data.

Acknowledgements

The authors are grateful to the Department of Soil Science (LSO) of ESALQ-USP for their support during this research, and to the members of Geotechnologies in the Soil Science Group (GEOCIS) (https://esalq-geocis.wixsite.com/english).

Funding

This work was supported by the São Paulo Research Foundation (FAPESP), Brazil [grant numbers: 2021/05129-8 and 2014/22262-0] and Ministerio de Ciencia, Tecnología e Innovación of Colombia Scholarship Program No. 860.

References

Acosta-Martinez, V., Zobeck, T.M., Allen, V., 2004. Soil microbial, chemical and physical properties in continuous cotton and integrated crop-livestock systems. Soil Sci. Soc. Am. J. 68 (2004), 1875–1884.

Adhikari, K., Hartemink, A.E., Minasny, B., Bou Kheir, R., Greve, M.B., Greve, M.H., Hui, D., 2014. Digital Mapping of Soil Organic Carbon Contents and Stocks in Denmark. PLoS One 9 (8), e105519.

Alvares, C.A., Stape, J.L., Sentelhas, P.C., De Moraes Gonçalves, J.L., Sparovek, G., 2013. Koppen's climate classification map for Brazil. Meteorol. Z. 22, 711–728. https://doi.org/10.1127/0941-2948/2013/0507.

Angers, D.A., Arrouays, D., Saby, N.P.A., Walter, C., 2011. Estimating and mapping the carbon saturation deficit of French agricultural topsoils. Soil Use ManagE. 27, 448–452.

Arrouays, D., Saby, N., Walter, C., Lemercier, B., Schvartz, C., 2006. Relationships betweenparticle-size distribution and organic carbon in French arable topsoils. Soil Use Manage. 22, 48–51.

Ashton, N., Tye, A., Pattrick, R., van Dongen, B., 2016. Carbon sequestration in the soils of Northern Ireland: potential based on mineralogical controls. In: Young, M.E. (Ed.), Unearthed: impacts of the Tellus surveys of the north of Ireland. Dublin, Royal Irish Academy.

Baldock, J.A., Skjemstad, J.O., 2000. Role of the soil matrix and minerals in protecting natural organic materials against biological attack. Org Geochem. 31 (7-8), 697–710.

Benites, V., Machado, P., Fidalgo, E., Coelho, M., Madari, B., 2007. Pedotransfer functions for estimating soil bulk density from existing soil survey reports in Brazil. Geoderma 139, 90–97.

Berg, M., Oliveira, J., 2000. Variability of apparently homogeneous soilscapes in São Paulo State, Brazil: II. Quality Of Soil Maps. R. Bras. Ci. Solo 24, 393–407.

Bigham, J.M., Fitzpatrick, R.W., Schulze, D., 2002. Iron oxides. In: Dixon, J.B., Schulze, D.G. (Eds.), Soil mineralogy with environmental applications. Soil Science Society of America Book Series, Madison, WI, USA, pp. 323–366.

Boddey, R.M., Jantalia, C.P., Conceição, P.C., Zanatta, J.A., Bayer, C., Mielniczuk, J., Dieckow, J., Santos, H.P., Denardin, J.E., Aita, C., Giacomini, S.J., Alves, B.J.R., Urquiaga, S., 2010. Carbon accumulation at depth in Ferralsols under zero-till subtropical agriculture. Glob. Chang. Biol. 16, 784–795.

Bonfatti, B.R., Demattê, J.A.M., Marques, K.P.P., Poppiel, R.R., Rizzo, R., Mendes, W., Silvero, N.E.Q., Safanelli, J.L., 2020. Digital mapping of soil parent material in a heterogeneous tropical area. Geomorphology 367, 107305. https://doi.org/10.1016/j.geomorph.2020.107305.

Bouyoucos, G.J., 1962. Hydrometer method improved for making particle size analysis of soils. Agron. J. 54, 464–465. https://doi.org/10.2134/agronj1962.00021962005400050028x.

Breiman, L., 2001. Random forests. Mach. Learn. 45 (2001), 5–32.

Brodowski, S., John, B., Flessa, H., Amelung, W., 2006. Aggregate- occluded black carbon in soil. Eur. J. Soil. Sci. 57, 539–546.

Carvalho, L., Moniz, R., Souza, E., Vieira, G., Schaefer, C., Fernandes, E., 2019. Modelling and mapping soil organic carbon stocks in Brazil. Geoderma 340 (2019), 337–350.

Chung, H., Grove, J.H., Six, J., 2008. Indications for soil carbon saturation in a temperate agroecosystem. Soil Sci. Soc. Am. J. 72, 1132–1139.

Churchman, G.J., Singh, M., Schapel, A., Sarkar, B., Bolan, N., 2020. Clay minerals as the key to the sequestration of carbon in soils. Clays Clay Miner. 68, 135–143.

Churchman, G.J., Velde, B., 2019. Soil Clays, Linking Geology, Biology, Agriculture, and the Environment. CRC Press, Boca Raton, Florida, USA.

Coelho, F., Giasson, E., Campos, A., Tiecher, T., Costa, J., Coblinski, J., 2020. Digital soil class mapping in Brazil: a systematic review. Soils and Plant Nutrition. Sci. agric. (Piracicaba, Braz.) 78 (5). https://doi.org/10.1590/1678-992X-2019-0227.

Cotrufo, M.F., Ranalli, M.G., Haddix, M.L., Six, J., Lugato, E., 2019. Soil carbon storage informed by particulate and mineral-associated organic matter. Nat. Geosci. 12 (12), 989–994. https://doi.org/10.1038/s41561-019-0484-6.

De Mastro, F., Traversa, A., Cocozza, C., Pallara, M., Brunetti, G., 2020. Soil Organic Carbon Stabilization: Influence of Tillage on Mineralogical and Chemical Parameters. Soil Syst. 4 (3), 58.

Demattê, J.A.M., Dotto, A.C., Paiva, A.F.S., Sato, M.V., Dalmolin, R.S.D., De Araújo, M.D. O.S.B., Da Silva, E.B., Nanni, M.R., Ten Caten, A., Noronha, N.C., Lacerda, M.P.C., De Araújo Filho, J.C., Rizzo, R., Bellinaso, H., Francelino, M.R., Schaefer, C.E.G.R., Vicente, L.E., Dos Santos, U.J., De Sá Barretto Sampaio, E.V., Menezes, R.S.C., De Souza, J.J.L.L., Abrahão, W.A.P., Coelho, R.M., Grego, C.R., Lani, J.L., Fernandes, A. R., Gonçalves, D.A.M., Silva, S.H.G., De Menezes, M.D., Curi, N., Couto, E.G., Dos Anjos, L.H.C., Ceddia, M.B., Pinheiro, É.F.M., Grunwald, S., Vasques, G.M., Marques Júnior, J., Da Silva, A.J., Barreto, M.C.D.V., Nóbrega, G.N., Da Silva, M.Z., De Souza, S.F., Valladares, G.S., Viana, J.H.M., Da Silva Terra, F., Horák-Terra, I., Fiorio, P.R., Da Silva, R.C., Frade Júnior, E.F., Lima, R.H.C., Alba, J.M.F., De Souza Junior, V.S., Brefin, M.D.L.M.S., Ruivo, M.D.L.P., Ferreira, T.O., Brait, M.A., Caetano, N.R., Bringhenti, I., De Sousa Mendes, W., Safanelli, J.L., Guimarães, C.C. B., Poppiel, R.R., E Souza, A.B., Quesada, C.A., Do Couto, H.T.Z., 2019. The Brazilian Soil Spectral Library (BSSL): A general view, application and challenges. Geoderma 354, 113793. https://doi.org/10.1016/j.geoderma.2019.05.043.

Demattê, J., Fongaro, C., Rizzo, C., Safanelli, J.L., 2018. Geospatial Soil Sensing System (GEOS3): a powerful data mining procedure to retrieve soil spectral reflectance from satellite images. Remote Sens. Environ. 212 (2018), 161–175.

Di Iorio, E., Circelli, L., Lorenzetti, R., Costantini, E., Perl, S., Colombo, C., 2019. Estimation of andic properties from Vis-NIR diffuse reflectance spectroscopy for volcanic soil classification. Catena 182 (2019), 104109.

Diekow, J., Mielniczuk, J., Knicker, H., Bayer, C., Dick, D.P., Kögel-knabner, I., 2005. Carbon and nitrogen stocks in physical fractions of a subtropical Acrisol as influenced by long-term no-till cropping systems and N fertilization. Plant and Soil 268, 319–328.

Dos Reis, C., Pinheiro, D., Caldas, J., Bayer, C., 2014. Carbon sequestration in clay and silt fractions of Brazilian soils under conventional and no-tillage systems. Soils and Plant Nutrition. Sci. agric. (Piracicaba, Braz.) 71 (4).

Duiker, S.W., Rhoton, F.E., Torrent, J., Smeck, N.E., Lal, R., 2003. Iron (hydr)oxide crystallinity effects on soil aggregation. Soil Sci. Soc. Am. J. 67, 606–611.

Elhorst, J.P. 2014. Spatial Econometrics: From Cross-sectional Data to Spatial Panels. Springer, Heidelberg New York Dordrecht London, http://www.springer.com/economics/regional+science/book/978-3-642-40339-2.

Eusterhues, K., Rumpel, C., Kogel-Knabner, I., 2005. Organo-mineral associations in sandy acid forest soils: importance of specific surface area, iron oxides and micropores. Eur. J. Soil Sci. 56, 753–763. https://doi.org/10.1111/j.1365-2389.2005.00710.x.

Feller, C., Beare, M.H., 1997. Physical control of soil organic matter dynamics in the tropics. Geoderma 79 (1–4), 69–116.

Feng, X., Simpson, A.J., Simpson, M., 2005. Chemical and mineralogical controls on humic acid sorption to clay mineral surfaces. Org. Geochem. 36, 1553–1566.

Follett, R., Kimble, J., Lal, R., 2001. In: The potential of US grazing lands to sequester soil carbon. Lewis Publishers, Boca Raton, Florida, pp. 401–430.

Freibauer, A., Rounsevell, M.D.A., Smith, P., Verhagen, J., 2004. Carbon sequestration in the agricultural soils of Europe. Geoderma 122, 1–23.

Fujisaki, K., Chapuis-Lardy, L., Albrecht, A., Razafimbelo, T., Chotte, J.L., Chevallier, T., 2018. Data synthesis of carbon distribution in particle size fractions of tropical soils:

Implications for soil carbon storage potential in croplands. Geoderma 313 (2018), 41–51.
Georgiou, K., Jackson, R.B., Vindušková, O., Abramoff, R.Z., Ahlström, A., Feng, W., Harden, J., Pellegrini, A., Polley, H., Soong, J., Riley, W., Torn, M.S., 2022. Global stocks and capacity of mineral-associated soil organic carbon. Nat. Commun. 13 (1), 3797.
Gray, J., Bishop, T., Wilson, B.R., 2015. Factors controlling soil organic carbon stocks with depth in Eastern Australia. Soil Sci. Soc. Am. J. 79 (6), 1741–1751.
Guzmán, G., Alcantara, E., Baron, V., Torrent, J., 1994. Phytoavailability of phosphate adsorbed on ferrihydrite, hematite, and goethite. Plant Soil 159 (219–225), 1994.
Hassink, J., 1997. The capacity of soils to preserve organic C and N by their association with clay and silt particles. Plant Soil 191 (1997), 77–87. https://doi.org/10.1023/A:1004213929699.
Hobley, E., Wilson, B., Wilkie, A., Gray, J., Koen, T., 2015. Drivers of soil organic carbon storage and vertical distribution in Eastern Australia. Plant Soil 390 (2015), 111–127.
Hoffland, E., Kuyper, T., Comans, R., Creamer, R., 2020. Eco-functionality of organic matter in soils. Plant Soiil 2020 (455), 1–22. https://doi.org/10.1007/s11104-020-04651-9.
Hoge, M., Wohling, T., Nowak, W., 2018. A primer for Model Selection: The Decisive Role of Model Complexity. Water Resour. Res. 54, 1688–1715. https://doi.org/10.1002/2017WR021902.
Houghton, R.A., 2003. Why are estimates of the terrestrial carbon balance so different? Glob. Chang. Biol. 9, 500–509.
Ingram, J., Fernandes, E.C.M., 2001. Managing carbon sequestration in soils: concepts and terminology. Agric. Ecosyst. Environ. 871, 111–117.
IUSS Working Group WRB. 2015. World Reference Base for Soil Resources 2014: International Soil Classification System for Naming Soils and Creating Legends for Soil Maps. FAO, Rome, Italy (2015).
Jindaluang, W., Kheoruenromne, I., Suddhiprakarn, A., Singh, B., Singh, B., 2013. Influence of soil texture and mineralogy on organic matter content and composition in physically separated fractions soils of Thailand. Geoderma 195–196 (2013), 207–219. https://doi.org/10.1016/j.geoderma.2012.12.003.
Johnson, J., Franzluebbers, A., Weyers, S., Reicosky, D., 2007. Agricultural opportunities to mitigate greenhouse gas emissions. Environ. Pollut. 150, 107–124.
Kaiser, K., Guggenberge, G., 2000. The role of DOM sorption to mineral surfaces in the preservation of organic matter in soils. Org Geochem. 31, 711–725.
Kaiser, K., Zech, W., 2000. Dissolved organic matter sorption by mineral constituents of subsoil clay fractions. J. Plant Nutr. Soil Sci. 163 (5), 531–535.
Kalbitz, K., Schwesig, D., Rethemeyer, J., Matzner, E., 2005. Stabilization of dissolved organic matter by sorption to the mineral soil. Soil Biol. Biochem. 37, 1319–1331.
Kämpf, N. & N. Curi. 2003. Argilominerais em solos brasileiros. In: CURI, N. *et al.*, Tópicos em ciência do solo. Viçosa: Sociedade Brasileira de Ciência do Solo, 2003. v.3. p.1-54.
Khaledian, Y., Miller, B.A., 2020. Selecting appropriate machine learning methods for digital soil mapping. Appl. Math. Model. 81, 401–418. https://doi.org/10.1016/j.apm.2019.12.016.
Kimble, J.M., Heath, L.S., Birdsey, R.A., Lal, R., 2003. The Potential of U.S. Forest Soils to Sequester Carbon and Mitigate the Greenhouse Effect. CRC Press, New York.
Kirsten, M., Mikkuta, R., Vogel, C., Thompson, A., Mueller, C., Kimaro, D., Bergsma, H., Feger, K., Kalbitz, K., 2021. Iron oxides and aluminous clays selectively control soil carbon storage and stability in the humid tropics. Sci. Rep. 11, 5076.
Kögel-Knabner, I., Guggenberger, G., Kleber, M., et al., 2008. Organo-mineral associations in temperate soils: integrating biology, mineralogy, and organic matter chemistry. J. Plant Nutr. Soil Sci. 171, 61–82.
Lal, R., 2004. Soil carbon sequestration impacts on global climate change and food security. Science 304 (2004), 1623–1627.
Lalonde, K., Mucci, A., Ouellet, A., Gélinas, Y., 2012. Preservation of organic matter in sediments promoted by iron. Nature 483, 198–200. https://doi.org/10.1038/nature10855.
Lamichhane, S., Kumar, L., Wilson, B., 2019. Digital soil mapping algorithms and covariates for soil organic carbon mapping and their implications: A review. Geoderma 352 (15), 395–413.
Liu, X., Chen, J., 2021. Variable Selection for the Spatial Autoregressive Model with Autoregressive Disturbances. Mathematics 9, 1448. https://doi.org/10.3390/math9121448.
Liu, X., Herbert, S.J., Hashemi, A.M., Zhang, X., Ding, G., 2006. Effects of agricultural management on soil organic matter and carbon transformation – a review. Plant Soil Environ. 52, 531–543. https://doi.org/10.17221/3544-PSE.
Loveland, P., Webb, J., 2003. Is there a critical level of organic matter in the agricultural soils of temperate regions: a review. Soil Tillage Res. 70, 1–18.
Marschner, B., Brodowski, S., Dreves, A., Gleixner, G., Gude, A., Grootes, P.M., Hamer, U., Heim, A., Jandl, G., Ji, R., 2008. How relevant is recalcitrance for the stabilization of organic matter in soils? J. Plant Nutr. Soil Sci. 171 (2008), 91–110.
McBratney, A., Santos, M., Minasny, B., 2003. On digital soil mapping. Geoderma 117 (2003), 3–52.
Mendes, W., Demattê, J.A.M., Bonfatti, B., Resende, M., Campos, L., Da Costa, A., 2021. A novel framework to estimate soil mineralogy using soil spectroscopy. Appl. Geochem. 127, 104909 https://doi.org/10.1016/j.apgeochem.2021.104909.
Mendez, C. 2020. Spatial regression analysis in R. R Studio/RPubs. Available at https://rpubs.com/quarcs-lab/tutorial-spatial-regression.
Minasny, B., McBratney, A., Malone, B.P., 2013. WheelerDigital mapping of soil carbon. Adv. Agron. 118 (2013), 1–47.
Minasny, B., Malone, B.P., McBratney, A.B., Angers, D.A., Arrouays, D., Chambers, A., Chaplot, V., Chen, Z.S., Cheng, K., Das, B.S., Field, D.J., Gimona, A., Hedley, C.B., Hong, S.Y., Mandal, B., Marchant, B.P., Martin, M., McConkey, B.G., Mulder, V.L., O'Rourke, S., Richer-De-forges, A.C., Odeh, I., Padarian, J., Paustian, K., Pan, G., Poggio, L., Savin, I., Stolbovoy, V., Stockmann, U., Sulaeman, Y., Tsui, C.C., Vågen, T.G., van Wesemael, B., Winowiecki, L., 2017. Soil carbon 4 per mille. Geoderma 292, 59–86. https://doi.org/10.1016/J.GEODERMA.2017.01.002.
Nave, E., Swanston, C., Mishra, U., Nadelhoffer, K.J., 2013. Afforestation effects on soil carbon storage in the United States: a synthesis. Soil Sci. Soc. Am. J. 77 (3), 1035–1047.
Oades, J., 1988. The retention of organic matter in soils. Biogeochemistry 5, 35–70.
Ogle, S.M., Breidt, F.J., Paustian, K., 2005. Biogeochemistry 72, 87. https://doi.org/10.1007/s10533-004-0360-2.
Okunlola, O.A., Alobid, M., Olubusoye, O.E., Ayinde, K., Lukman, A., Szucs, I., 2021. Spatial regression and geostatistics discourse with empirical application to precipitation data in Nigeria. Sci. Rep. 11, 16848. https://doi.org/10.1038/s41598-021-96124-x.
Padarian, J., Minasny, B., Mcbratney, A., 2019. Using deep learning for digital soil mapping. Soil 5 (1), 79–89. https://doi.org/10.5194/soil-5-79-2019.
Padarian, J., Minasny, B., Mcbratney, A.B., 2020. Machine learning and soil sciences: A review aided by machine learning tools. Soil 6, 35–52. https://doi.org/10.5194/soil-6-35-2020.
Padarian, J., Minasny, B., McBratney, A., Smith, P., 2022. Soil carbon sequestration potential in global croplands. PeerJ 10, e13740.
Paustian, K., Andren, O., Janzen, H., et al., 1997. Agricultural soils as a sink to mitigate CO2 emissions. Soil Use Manag. 13, 230–244.
Percival, H.J., Parfitt, R.L., Scott, N., 2000. Factors controlling soil carbon levels in New Zealand grasslands: Is clay content important? Soil Sci. Soc. Am. J. 64, 1623–1630.
Poeplau, C., Don, A., 2013. Sensitivity of soil organic carbon stocks and fractions to different land-use changes across Europe. Geoderma 192 (2013), 189–201.
Prout, J.M., Shepherd, K.D., McGrath, S.P., Kirk, G.J., Haefele, S.M., 2021. What is a good level of soil organic matter? An index based on organic carbon to clay ratio. Eur. J. Soil Sci. 72 (6), 2493–2503. https://doi.org/10.1111/ejss.13012.
Rabbi, S., Tighe, M., Delgado-Baquerizo, M., Cowie, A., Robertson, F., Dalal, R., Page, K., Crawford, D., Wilson, B., Schwenke, G., Mcleod, M., Badgery, W., Dang, Y., Bell, M., O'leary, G., Liu, D., Baldock, J., 2015. Climate and soil properties limit the positive effects of land use reversion on carbon storage in Eastern Australia. Sci. Rep. 5, 17866.
Rasmussen, C., Matsuyama, N., Dahlgren, R.A., Southard, R.J., Brauer, N., 2007. Soil genesis and mineral transformation across and environmental gradient on andesitic lahar. Soil Sci. Soc. Am. J. 71, 225–237.
Rodrigues, L., Dieckow, J., Giacomini, S., Ottonelli, A., Zorzo, G., Bayer, C., 2022. Carbon sequestration capacity in no-till soil decreases in the long-term due to saturation of fine silt plus clay-size fraction. Geoderma 412 (2022), 115711.
Sabetizade, M., Gorji, M., Roudier, P., Zolfaghari, A.A., Keshavarzi, A., 2021. Combination of MIR spectroscopy and environmental covariates to predict soil organic carbon in a semi-arid region. Catena 196, 0341–8162. https://doi.org/10.1016/j.catena.2020.104844.
Saidy, A.R., Smernik, R.J., Baldock, J.A., Kaiser, K., Sanderman, J., 2013. The sorption of organic carbon onto differing clay minerals in the presence and absence of hydrous iron oxide. Geoderma 209–10, 15–21.
Sauerbeck, D., 2001. CO_2 emissions and C sequestration by agriculture – perspective sand limitations. Nutr. Cycl. Agroecosyst. 60, 253–266.
Schaefer, C., Fabris, J.D., Ker, J.C., 2008. Minerals in the clay fraction of Brazilian Latosols (Oxisols): a review. Clay Miner. 43 (137–154), 2008.
Shi, Z., Ji, W., Viscarra Rossel, R., Chen, S. & Y. Zhou. 2015. Prediction of soil organic matter using a spatially constrained local partial least squares regression and the Chinese vis-NIR spectral library Eur. J. Soil Sci., 66 (4) (2015), pp. 679-687.
Singh, M., Sarkar, B., Sarkar, S., Churchman, J., Bolan, N., Mandal, S., Menon, M., Purakayastha, T.J., Beerling, D.J., 2018. Stabilization of soil organic carbon as influenced by clay mineralogy. Adv. Agron. 148, 33–84.
Six, J., Conant, R., Paul, E. & K. Paustian. 2002. Stabilization mechanisms of soil organic matter: implications for C-saturation of soils Plant Soil, 241 (2002), pp. 155-176.
Smith, P., 2004. Carbon sequestration in croplands: the potential in Europe and theglobal context. Eur. J. Agron. 20, 229–236.
Smith, P., 2012. Agricultural greenhouse gas mitigation potential globally, in Europeand in the UK: what have we learnt in the last 20 years? Glob. Chang. Biol. 18, 35–43.
Soil Science Division Staff, 2017. Soil survey manual. In: Ditzler, C., Scheffe, K., Monger, H.C. (Eds.), Agriculture Handbook 18, 4th ed. Government Printing Office, Washington, D.C. Retrieved May 26, 2020, from.
Sollins, P., Homann, P., Caldwell, B., 1996. Stabilization and destabilization of soilorganic matter: mechanisms and controls. Geoderma 74, 65–105.
Sothe, C., Gonsamo, A., Arabian, J. & J. Snider. 2022. Large scale mapping of soil organic carbon concentration with 3D machine learning and satellite observations. Geoderma Volume 405, 1 January 2022, 115402.
Stewart, C., Paustian, K., Conant, R., Plante, A., Six, J., 2008. Soil carbon saturation: evaluation and corroboration by long-term incubations. Soil Biol. Biochem. 40, 1741–1750.
Tayebi, M., Fim Rosas, J.T., Mendes, W.D.S., Poppiel, R.R., Ostovari, Y., Ruiz, L.F.C., Dos Santos, N.V., Cerri, C.E.P., Silva, S.H.G., Curi, N., Silvero, N., Demattê, J.A.M., 2021. Drivers of Organic Carbon Stocks in Different LULC History and along Soil Depth for a 30 Years Image Time Series. Remote Sens. 2021 (13), 2223. https://doi.org/10.3390/rs13112223.
Teng, H., Viscarra, R., Shi, A., Behrens, T., 2018. Updating a national soil classification with spectroscopic predictions and digital soil mapping. Catena 164 (2018), 125–134.
USGS. 2018. USGS EROS archive - digital elevation - Shuttle radar Topography mission (SRTM) 1 arc-second global [WWW document] Earth Resour. Obs. Sci. Cent https://doi-org.ezproxy.unal.edu.co/10.5066/F7PR7TFT (2018) Wang *et al.*, 2020.

Vleeshouwers, L., Verhagen, A., 2002. Carbon emission and sequestration byagricultural land use: a model study for Europe. Glob. Chang. Biol. 8, 519–530.
von Lützow, M., Kögel-Knabner, I., Ekschmitt, K., Matzner, E., Guggenberger, G., Marschner, B., Flessa, H., 2006. Stabilization of organic matter in temperate soils: mechanisms and their relevance under different soil conditions—a review. Eur. J. Soil Sci. 57 (2006), 426–445.
Walkley, A., Black, I.A., 1934. An examination of the Degtjareff method for determining soil organic matter, and proposed modification of the chromic acid titration method. Soil Sci. 37, 29–38.
Weber, K.A., Achenbach, L.A., Coates, J., 2006. Microorganisms pumping iron: anaerobic microbial iron oxidation and reduction. Nat. Rev. Microbiol. 4, 752–764. https://doi.org/10.1038/nrmicro1490.
Webster, R., Oliver, M., 2007. Geostatistics for Environmental Scientists. Editorial Jhon Wiley & Sons, Ltd, p. 333.
Weil, R., Brady, N.C., 2016. The Nature and Properties of Soils (15th edition),. Pearson Education.
Wen, Y., Xiao, J., Goodman, B., He, X., 2019. Effects of Organic Amendments on the Transformation of Fe (Oxyhydr)Oxides and Soil Organic Carbon Storage. Front. Earth Sci. 7, 2019. https://www.frontiersin.org/article/10.3389/feart.2019.00257.
Wiesmeier, M., Barthold, F., Blank, B., Kögel-Knabner, I., 2011. Digital mapping of soil organic matter stocks using Random Forest modeling in a semi-arid steppe ecosystem. Plant Soil 340 (1–2), 7–24.
Wiesmeier, M., Hubner, R., Barthold, F., et al., 2013. Amount, distribution and drivingfactors of soil organic carbon and nitrogen in cropland and grassland soils ofsoutheast Germany (Bavaria). Agr Ecosyst Environ 176, 39–52.
Yang, L., Li, X., Shib, J., Shen, F., Qi, F., Gao, B., Chen, Z., Zhu, A., Zhou, C., 2020. Evaluation of conditioned Latin hypercube sampling for soil mapping based on a machine learning method. Geoderma 369 (2020), 114337.
Yang, Y., Shen, Z., Bisset, A., Viscarra Rossel, R., 2021. Estimating soil fungal abundance and diversity at a macroecological scale with deep learning spectrotransfer functions. Soil Discuss. [preprint], doi: 10.5194/soil-2021-79, in review.
Zeraatpishe, M., Khormali, F., 2012. Carbon stock and mineral factors controlling soil organic carbon in a climatic gradient, Golestan province. J. Soil Sci. Plant Nutr. 12 (4), 637–654.
Zeraatpisheh, M., Jafari, A., Bodaghabadi, M.B., Ayoubi, S., Taghizadeh-Mehrjardi, R., Toomanian, N., Kerry, R., Xu, M., 2020. Conventional and digital soil mapping in Iran: past, present, and future. Catena 188, 104424.